Ground-based Near-Infrared Observations of the Venus Night Side: Near-Infrared $0_2(^1\Delta)$ Airglow from the Upper Atmosphere

D. Crisp (Jet Propulsion Laboratory), V. S. Meadows (University of Sydney and Anglo-Australian Observatory)[1], B. Bezard, C. de Bergh (Observatory of Paris-Meudon), J.-P. Maillard (IAP Paris), and F. P. Mills (Caltech)

[1] *present affiliation; National Research Council Resident Research Associate, Jet Propulsion Laboratory.*

ABSTRACT

The new-infrared $O_2(a^1\Delta_g)$ airglow emission from the Venus mesopause ($\sim$ 100 km) is surprisingly intense and variable. Spectroscopic observations acquired in 1975 indicated day and nightside emission rates of 1.5 and 1.2 Mega-Rayleigh (1 MR = 1012 photons $cm^{-2}s^{-1}$ into 4π steradians). The observed airglow intensities are puzzling because they indicate that more than half of the atomic oxygen that is produced through the photolysis of CO_2 on the day side of Venus must recombine to produce 0_2 in the excited ($a^1\Delta_g$) state. Existing laboratory measurements indicate that this reaction should have quantum efficiencies no larger than a few percent. More recent observations reveal even larger $O_2(a^1\Delta_g)$ airglow intensities (> 5 MR) as well as dramatic spatial and temporal variations in this airglow. High resolution (0.3 cm^{-1}) spectra of the Venus night side obtained with the Canada France Hawaii Telescope Fourier Transform Spectrometer in 1991 confirm that $O_2(a^1\Delta_g)$ intensities greater than 1 MR are common and indicate rotational temperatures of 186 ± 6 K in the emitting layer. Spectral image cubes taken with the Anglo-Australian Telescope/InfraRed Imaging Spectrometer and the Canada France Hawaii Telescope Imaging Fourier Transform Spectrometer during 1991, 1993, and 1994 provide a more complete description of the spatial and temporal variability in this emission. Images extracted at wavelengths within the $O_2(a^1\Delta_g)$ Q-branch (1.269 μm) often show contrasts larger than 10 to 1 across the night side. Even though the disk-averaged intensity is comparable to that seen in 1975, some localized regions are more than five times as bright. The brightest emission is often confined to 1000-2000 km diameter spots at low latitudes, at local times between midnight and 3 AM. The intensity of these spots can change by 20% in less than 1 hour, and they can vanish entirely in less than one day. These observations are being used to derive a more complete description of the chemistry and dynamics of the upper mesosphere of Venus.

1 Introduction

Ground-based spectroscopic observations of Venus acquired in 1975 revealed intense 1.27 μm $O_2(a^1\Delta_g)$ airglow emission from both the day and night sides of the planet. *Connes et al.* [1979] used the Fourier Transform Spectrometer (FTS) on the Palomar 5-m Hale telescope to take high-resolution ($\lambda/\Delta\lambda \sim$ 400,000) spectra of large (5 x 10 arc-second) regions of the 20

arc-second (") disk. Averages of spectra taken during 6 nights in November and December indicated dayside and nightside emission rates of 1.5 ± 0.3 and 1.2 ± 0.3 MR. These large intensities were surprising, because they indicated that the near-infrared airglow was about 1000 times brighter than the visible O_2 airglow detected by the *Venera* 9 and *10* probes [*Krasnopol'sky* 1983]. *Connes et al.* concluded that this near-infrared airglow was primarily a consequence of the recombination of atomic oxygen that is produced by the UV photolysis of CO_2 on the day side of Venus. The direct 2-body recombination of oxygen atoms is spin forbidden, but O-O bonds can be formed by 3-body and catalytic reactions (Table 1) that are sufficiently exothermic to produce O_2 in the excited ($0^1\Delta_g$) state. The airglow is then produced (within $\sim$ 3800 s) when each molecule emits a photon at wavelengths near 1.27 μm and returns to its ground state [*Krasnopol'sky* 1983]. Atmospheric chemistry models indicate that the majority of this airglow is produced in the upper mesosphere and lower thermosphere of Venus ($\sim$ 90-115 km), because collisional quenching dominates radiative de-excitation at lower altitudes [*Connes et al.* 1979; *Yung and Demore* 1 982; *Bougher and Borucki* 1994]. The similarity of the measured day and nightside intensities suggested that, unlike in the atmospheres of Earth and Mars, ozone photolysis plays a relatively minor role in the production of the $O_2(a^1\Delta_g)$ airglow, ,since this mechanism works only on the day side. The brightness of the nightside emission, and the relatively short lifetime of atomic oxygen at these levels ($\sim$ 1 day at 90 km) were interpreted as evidence for rapid transport, from the day to the night sides of the planet [*Connes et al.* 1979], These conclusions have been reinforced by Pioneer Venus observations [*Seiff et al. 1980, Taylor et al. 1980]* and by chemical and dynamical models of the Venus atmosphere [cf. *Yung and Demore*, 1982; *Bougher and Borucki 1994].*

The near-i]lfrarcd 0_2 airglow intensities recorded by *Connes et al.* arc still puzzling, however, because they imply globally-integrated $O_2(a^1\Delta_g)$ production rates comparable to the CO_2 photo-dissociation rates in the Venus atmosphere. *Yung and Demore* [1982] assumed $O_2(a^1\Delta_g)$ quantum yields near 66% in their model, and derived airglow intensities only about half as large as those observed. Recent laboratory measurements of $O_2(a^1\Delta_g)$ production rates have only added to this apparent deficit because they indicate $0_2(a^1\Delta_g)$ quantum yields of only a few percent for the reactions listed in Table 1 [*Leu et al. 1987].* These results have both raised doubts about the accuracy of the calibration of the observed intensities [*Yung and Demore 1982; Leu et al.* 1987] and motivated searches for other chemical mechanisms to produce this airglow. For example, *Leu et al.* [1987] proposed that the photolysis of $S0_2$ could provide an adequate source of atomic oxygen if the nominal mesospheric SO_2 mixing ratios (assumed to be $\sim$ 0.1 ppm) were enhanced by about a factor of 100 at the time *Connes et al.* made their measurements. This hypothesis could not be tested directly, because the first measurements of $S0_2$ in the Venus atmosphere were not made until several years after the O_2 airglow was observed [Barker 1 **979].**

To address these issues, and provide improved constraints on the chemistry and dynamics of this part of the Venus atmosphere, we acquired new near-infrared imaging and spectroscopic observations of Venus in 1990, 1991, 1993, and 1994. These observations not only confirmed that disk-averaged $O_2(a^1\Delta_g)$ intensities exceeding 1 MR are common [*Meadows*, 1994], they also revealed dramatic spatial and temporal variations in the airglow on the night side of

'J'able 1: Photodissociation and Recombinant ion Reactions for $O_2(a^1\Delta_g)$

Photodissociation Reaction:

$$CO_2 + h\nu \rightarrow CO + O$$

Recombination Reactions:[1,2]

$$O + O + M \rightarrow O_2 + M + 4.19\,eV$$
$$Cl + O_3 \rightarrow ClO + O_2(a^1\Delta_g) + 0.69\,eV$$
$$O + ClO \rightarrow Cl + O_2(a^1\Delta_g) + 1.41\,eV$$
$$H + O_2 + O \rightarrow OH + O_2(a^1\Delta_g) + 1.31\,eV$$

[]] Rothman (1 982). [2] National Institute of Standards and Technology (NIST), Standard Reference Database 25, "Structure and Properties version 2.02", January 1994.

Venus [Crisp *et* al. 1991; *Allen et al. 1992].* The background airglow intensities on the night side vary from almost zero to values like those recorded by *Connes et al. [1* **979],** but some isolated regions arc about 5 times as bright. The brightest regions arc often located at low latitudes just to the west of the anti-solar point (downwind, assuming retrograde zonal flow) or on the limb. These bright. regions have lifetimes of about one da-y. A complete description of these observations is included in section 2.

To derive $O_2(a^1\Delta_g)$ production rates from the observed airglow intensities, the observations must be corrected for viewing-angle effects and reflection from the underlying sulfuric acid cloud tops. To avoid confusion between the observed intensities and inferred O_2 production rates, wc have expressed the observed airglow radiances in SI units ($mW\,m^{-2}\,sr^{-1}$). For reference, *Connes et al. [1979]* reported observed intensities for the day and night sides of Venus as 4.3 and 3.4 MR. These intensities correspond to 0.54 and 0.43 $mW\,m^{-2}\,sr^{-1}$. The factors needed to obtain O_2 emission rates from the observed radiances arc derived in section 3.1. The inferred emission rates arc then in MR to fa cilitate comparisons with earlier work.

The physical and chemical processes that arc responsible for the observed spatial and temporal variations in the $O_2(a^1\Delta_g)$ airglow arc not yet understood, but these observations should eventually provide additional insight into the chemistry and dynamics of the upper atmosphere of Venus. For example, the dynamics at these levels are thought to be characterized by the superposition of a sub-solar to anti-solar (SSAS) flow and a weaker zonal flow [*Dickinson and Ridley, 1977; Shah et al. 1991; Goldstein et al. :1991; LC1 1OUCIL et al.* 1994; *Bougher and Borucki* 1 994]. The brightest- regions of'02 airglow on the night side might be associated with the locations of maximum subsidence since these regions have the largest atomic oxygen suppl y rates from the day side [*Crisp et al.* 1991; *Allen et al. 1992].* The observed local time of these bright regions would then provide constraints on the relative

strengths of the SSAS and zonal components of the circulation [*Bougher and Borucki 1994*]. The observed variability might be associated with gravity-wave-induced turbulence at these altitudes, like that proposed by *Alexander* [1992], or the availability of trace constituents that are essential to the production of $O_2(a^1\Delta_g)$, or other processes. These possibilities are explored in greater detail in Section 4.

2 *New* $O_2(a^1\Delta_g)$ Airglow Observations

New observations of the 1.27 μm O_2 airglow from the day and night sides of Venus were collected from ground-based observatories in Hawaii and Australia before and/or after the Venus inferior conjunctions in January 1990, August 1991, April 1993, and November 1994. This section summarizes the principal results from these observing programs, and compares these results to those reported by *Connes et al.* [1979] and those collected by the Galileo Near infrared Mapping Spectrometer (NIMS) during the 10 February 1990 Venus flyby [*Drossart et al. 1993*]. We focus our discussion on the airglow emission from the night side of the planet because the dayside airglow is much more difficult to discriminate from the reflected sunlight, and because the mechanisms that produce the nightside airglow are less well understood.

2.1 February 1990 AAT/FIGS observations:

Ground-based spectroscopic observations of the Venus night side were obtained with the Fabry-Perot, Infrared Grating Spectrometer (FIGS) at the Anglo-Australian Telescope (AAT) on 10 February 1990, just before the Galileo Venus Encounter [*Allen 1990; Crisp et al. 1991*]. The AAT/FIGS spectra have low to moderate spectral resolution ($\lambda/\Delta\lambda \sim 600$ to 1280), but high spatial resolution (1.4" aperture on a 49" disk). A low-resolution spectrum taken near the sub-Earth point on February 10 revealed a weak 1.269 μm O_2 $(a^1\Delta_g)$ airglow feature superimposed on a broader, deep-atmosphere thermal emission window, centered near 1.28 μm ([Crisp *et al.* 1991]; Figure 1). The Galileo NIMS experiment detected somewhat brighter O_2 emission in an isolated region of the night side at about 39 S latitude on the same day [*Drossart et al,* 1993]. A moderate-resolution AAT/FIGS nightside spectrum taken on 13 February more clearly discriminated the $O_2(a^1\Delta_g)$ from the deep-atmosphere thermal emission feature (Figure 2). The spectrally-integrated intensity of the O_2 Q-branch was ~ 0.18 mW m^{-2} sr^{-1}. The Q-branch accounts for $\sim 60\%$ of the total band strength (in local thermodynamic equilibrium). These results therefore indicate band-integrated (P-, Q-, and R-branch) intensities near 0.3 mW m^{-2} sr^{-1}. The intensity of the O_2 emission detected in the low-resolution FIGS spectrum from 10 February was very difficult to determine directly, but comparisons with a smoothed version of the 13 February FIGS spectrum indicates similar emission rates (Figure 1).

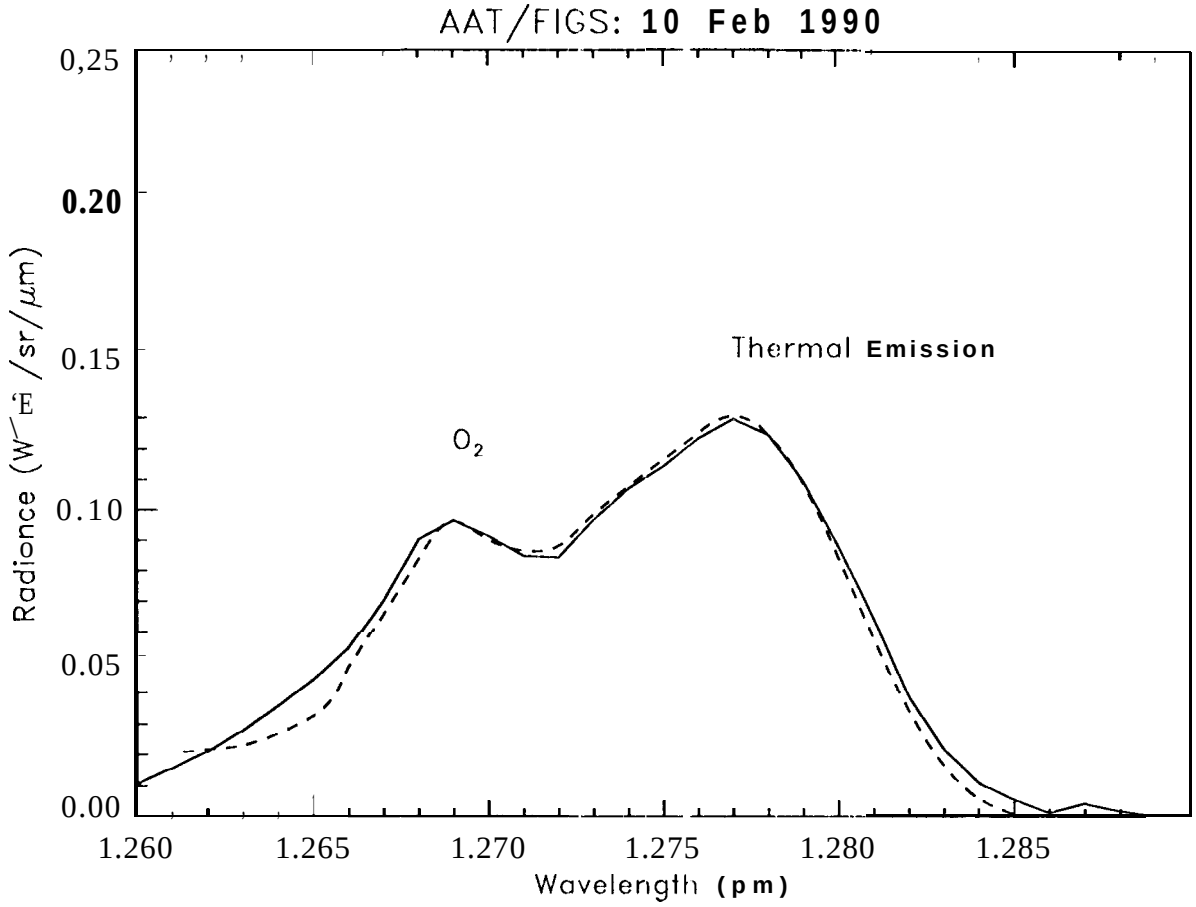

Figure 1: Low- resolution ($\lambda/\Delta\lambda \sim 600$) spectrum of the Venus night side taken with AAT/FIGS on 10 February, 1990 (solid line). The emission maximum centered at 1.277μm is a spectral window that allows thermal radiation to escape from altitudes between 15 and 25 km. The Q-branch of the $O_2(a^1\Delta_g)$ airglow band appears as a small bump on the shoulder of this window at 1.269pm. The dashed line shows a version of the moderate-resolution ($\lambda/\Delta\lambda \sim 1\,280$) AAT/FIGS spectrum from 13 February, 1990 that has been smoothed and scaled to match the 10 February spectrum at the peak of the 1.277μm thermal emission window. This comparison indicates that the O_2 airglow intensities were comparable in these two spectra.

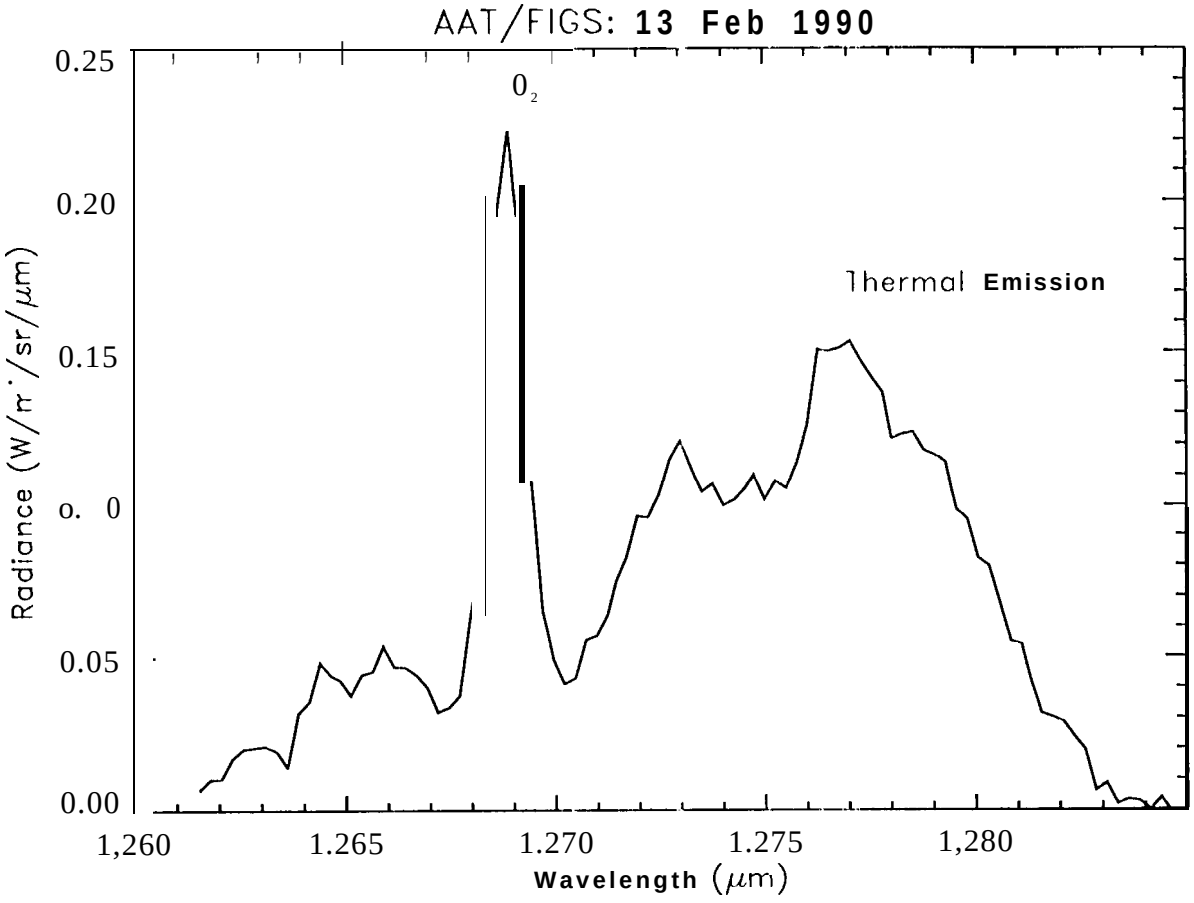

Figure 2: Moderate resolution ($\lambda/\Delta\lambda \sim$ 1280) spectrum of the Venus night side taken with AAT/FIGS on 13 February, 1990. The O_2 Q-branch at 1.269μm is more easily distinguished from the 1.277pm thermal emission window at this resolution.

2.2 June 1991 Cl? HT/FTS observations:

High resolution spectra of selected regions of the day and night sides of Venus were obtained with the Fourier Transform Spectrometer (FTS) on the Canada- France-Hawaii Telescope (CFHT) on 27 June and 1 July 1991. A 5" circular entrance aperture was used, and the angular size of Venus was $\sim$ 28". Spectra taken on 27 June have low signal-to-noise (S/N) because they were acquired on a sunlit sky, just as the eruption cloud from Mount Pinatubo began to pass overhead. We therefore smoothed these spectra with a triangular slit function with a full-width-at half-maximum (FWHM) of 1 cm^{-1} to yield an effective spectral resolution of $\lambda/\Delta\lambda \sim 7880$ (Figure 3). In spite of their modest S/N, these observations provided the first direct evidence for significant spatial variations in the $0_2(o\,^1\Delta_g)$ airglow on the night side of Venus. Observations centered near 10 N, 5 N, and 10 S latitude revealed airglow intensities that differed by a factor of 4. CFHT/FTS spectra of the Venus day and night sides were also taken on July 1. Unlike the earlier spectra, these obser vations were taken after sunset and have much higher S/N ($\sim$ 40; Figure 3). The high-resolution ($\lambda/\Delta\lambda \sim$ 7880) nightside spectrum taken at $\sim$15S latitude clearly resolves individual oxygen emission lines in the P- and R- branches of the $O_2(a^1\Delta_g)$ band near 1.269 μm. The spectrally-integrated O_2 airglow intensity exceeds 1.1 $mW\,m^{-2}\,sr^{-1}$. This was about six times brighter than that seem on 27 June, and about a factor of 2 larger than the nightside average values reported by *Connes et al.* [1979]. Comparisons of intensities of individual rotational transitions in the P- and R--branches of this emission spectrum indicated rotational temperatures of 186±6 K (Figure 4) in the emitting layer [*Crisp et al.* 1992]. This temperature is comparable to that derived by *Connes et al.* [1 979], (18.5+15 K).

2.3 July 1991 AAT/IRIS observations:

The first s~mtially-resolved images of the 0_2 airglow on the night side of Venus were taken with the InfraRed Imaging Spectrometer (IRIS) on the Anglo Australian Telescope (AAT) in July 1991 [*Allen et al.* 1992]. IRIS is a near-infrared camera/spectro meter with a 128 **x 128** (NICMOS2) detector [*Gillingham and Lankshear 1990; Allen et al.* 1993; *Meadows* 1994; *Meadows and Crisp, this issue].* We used the J-band (0.9 1.317 μm) echelle grism aud a 1.4 x 12" slit to produce spatially resolved spectra with a spectral resolution of $\lambda/\Delta\lambda \sim$ 400, and spatial resolution of 0.8''/pixcl. Spectral image cubes were compiled by allowing Venus to drift perpendicular to the slit, while recording spectra at slit positions separated by 0.6". Several "drift-scans" are combined to produce a full-disk image of Venus.

Figure 5 shows the spatial distribution of the $O_2(a^1\Delta_g)$ airglow observed on 27 and 28 July. The Venus disk was $\sim$ 42" in diameter, its phase was $\sim$ 0.18, and the sub-Earth point was in the evening hemisphere of the pl anet. The 27 July image was derived from the spectral image cubes described by *Allen et al.* [1992], but this image has been processed further to *(i)* remove contributions from the deep-atmosphere thermal emission, *(ii)* combine the emission from the P-, Q-, and R-branches of the $O_2(a^1\Delta_g)$ band, and *(iii)* provide an improved absolute radiometric calibration *[Meadows 1994].* On this date, the Venus night

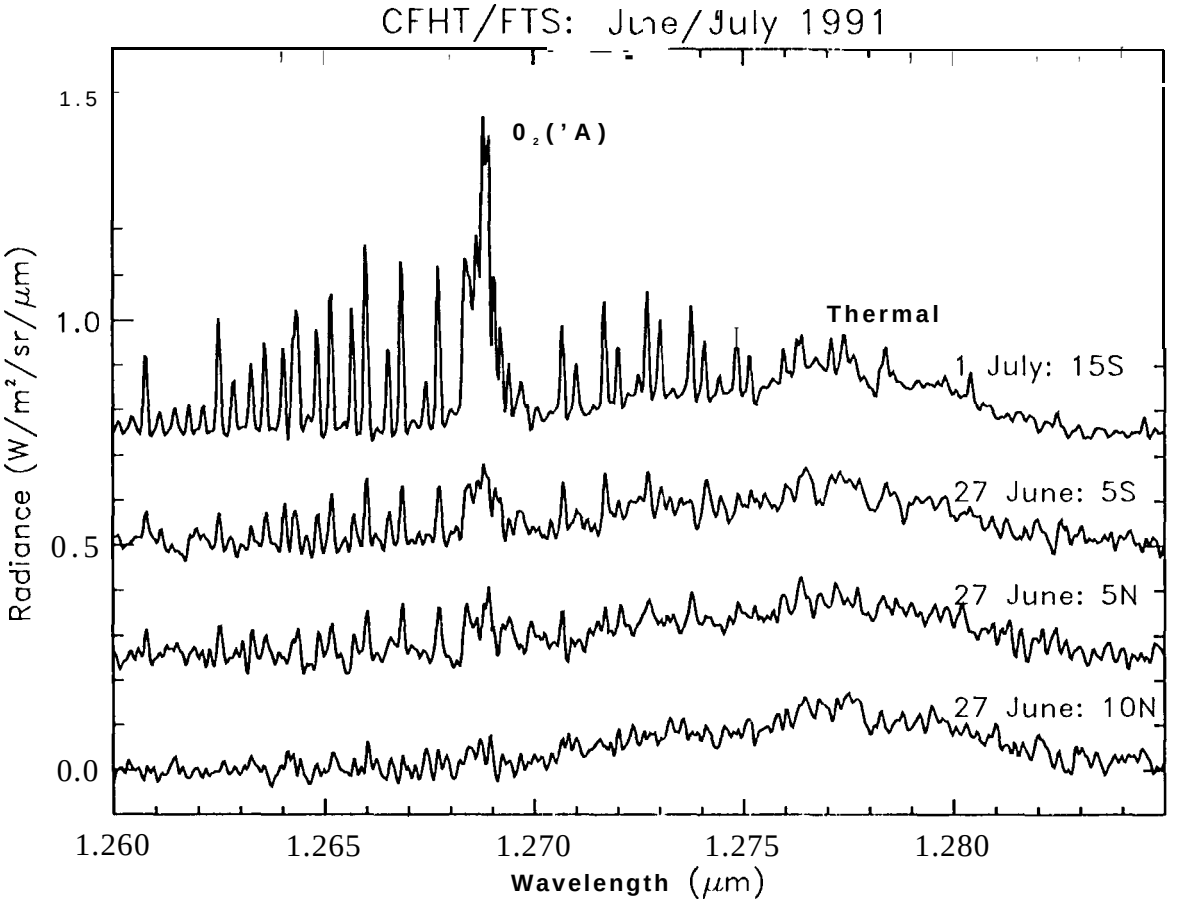

Figure 3: *CFHT/FTS spectra illustrating the spectral structure and variability of the* $O_2(^1$A) *airglow emission. These spectra are offset by 0.2 W* m^{-2} sr^{-1} μm^{-1} *for clarity. The bottom 3 spectra were acquired by centering the 5 arcsec aperture at points near 10 N (bottom), 5 N (middle), and 5 S (top) latitude, near -the sub-earth meridian on 27 June 1991. The top spectrum was taken at 15S on 1 July 1991. The lowest spectrum shows little* O_2 *airglow. A t this resolution, individual transitions in the 1'- and R- branches of the* $O_2(a^1\Delta_g)$ *band are clearly resolved from the thermal emission window centered near 1. 277* μm.

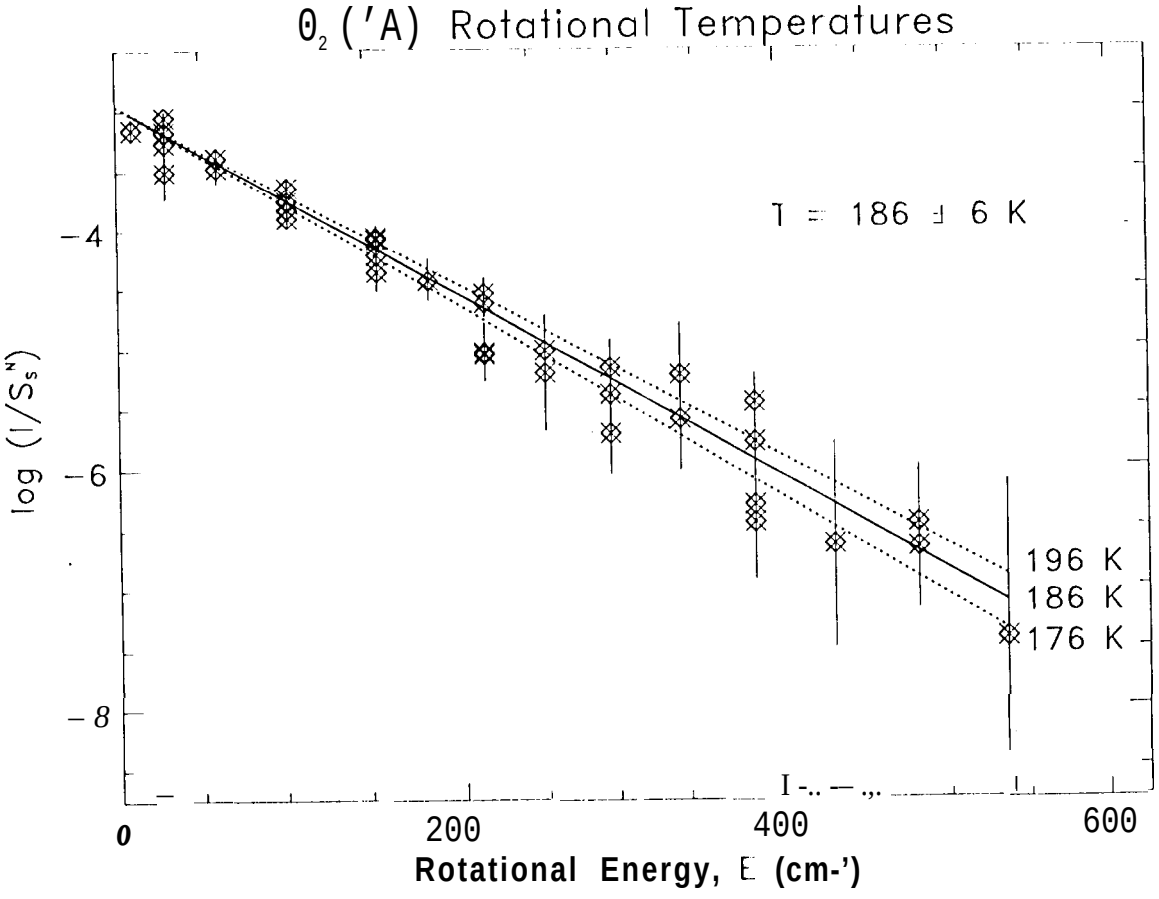

Figure 4: *Plots of rotational energy vs line intensity for the $O_2(a^1\Delta_g)$ emission from a CFHT/FTS spectrum acquired on 1 July 1991. The slope of this line indicates the mean rotational temperature of the emitting layer.*

side was characterized by localized regions of intense airglow with characteristic dimensions of $\sim$1000 km. The brightest feature was on the limb at $\sim$ 2AM local time. This feature had a spectrally-integrated (P-, Q- and R-branch) O_2 emission rate of 2.73: 0.2 mW m^{-2} sr^{-1}, but its apparent intensity was enhanced by limb brightening. A somewhat less intense discrete feature, with an intensity of 1.8 $\pm$ 0.2 mW $m^{-2}sr^{-1}$ was observed near the antisolar point. Dark regions with little or no O_2 airglow appear to radiate outward from the antisolar point. Low- resolution ($\lambda/\Delta\lambda \sim$ 300) IRIS spectra indicate that the nightside emission is dominated by thermal radiation from the deep atmosphere in these dark regions (Figure 6). These bright and dark regions were superimposed on a diffuse background emission, with mean intensities that varied from less than 0.1 to more than 0.5 mW m^{-2} sr^{-1}. Only one drift-scan of the Venus dark limb was obtained on 28 July 1 WI, due to bad weather. This scan showed significant changes in the O_2 intensity and distribution on the night side. The bright emission on the limb had vanished, and the brightest airglow was now located closer to the anti-solar point (Figure 5).

To compare these airglow intensities to those reported by Connes *et al.* (1979), we averaged the AAT/IRIS results over areas comparable to those sampled by their entrance aperture ($\sim$15% of the disk). For July 27, average intensities between 0.25 and 0.47 mW m^{-2} sr^{-1} were obtained for different aperture positions. When the averaging window was expanded to cover most of night side (excluding the limb and regions near the bright crescent), the average $O_2(a^1\Delta_g)$ intensity was 0.44 $\pm$ 0.06 mW m^{-2} sr^{-1}, in excellent agreement with the results published by Connes *et al.* The AAT/IRIS observations t aken on 28 July covered only 21% of the disk, but indicated average nightside O_2 intensities of 0.53 $\pm$ 0.05 mW m^{-2} sr^{-1}.

2.4 September 1991 AAT/IRIS observations:

AAT/IRIS observations of $O_2(a^1\Delta_g)$ emission from the Venus night side were also taken 011 17-20 September 1991, when the sub-Earth point was in the morning hemisphere (Figure 7). observations acquired at 0029 UT on 17 September show weak airglow activity, and very little contrast across the night side. Bad weather precluded observations on 18 September, but the AAT/IRIS image cubes taken on the 19th revealed intense emission in a region $\sim$ 1000 km in length, at low latitudes between 0100 and 0200 local time on Venus. Image cubes taken about one hour apart show that this emission had brightened by 20%, although it had not changed position appreciably. By 20 September, the brightest regions of emission had disappeared, leaving the overall intensity of the O_2 airglow less than that recorded on the 17tJll .

2.5 October 1991 AAT/IRIS observations:

Observations of nightside O_2 airglow were taken from the AAT and from the CFHT during October of 1991. The AAT/IRIS observations were not as photogenic as those taken earlier that year because Venus was well past opposition, and its apparent diameter had decreased to

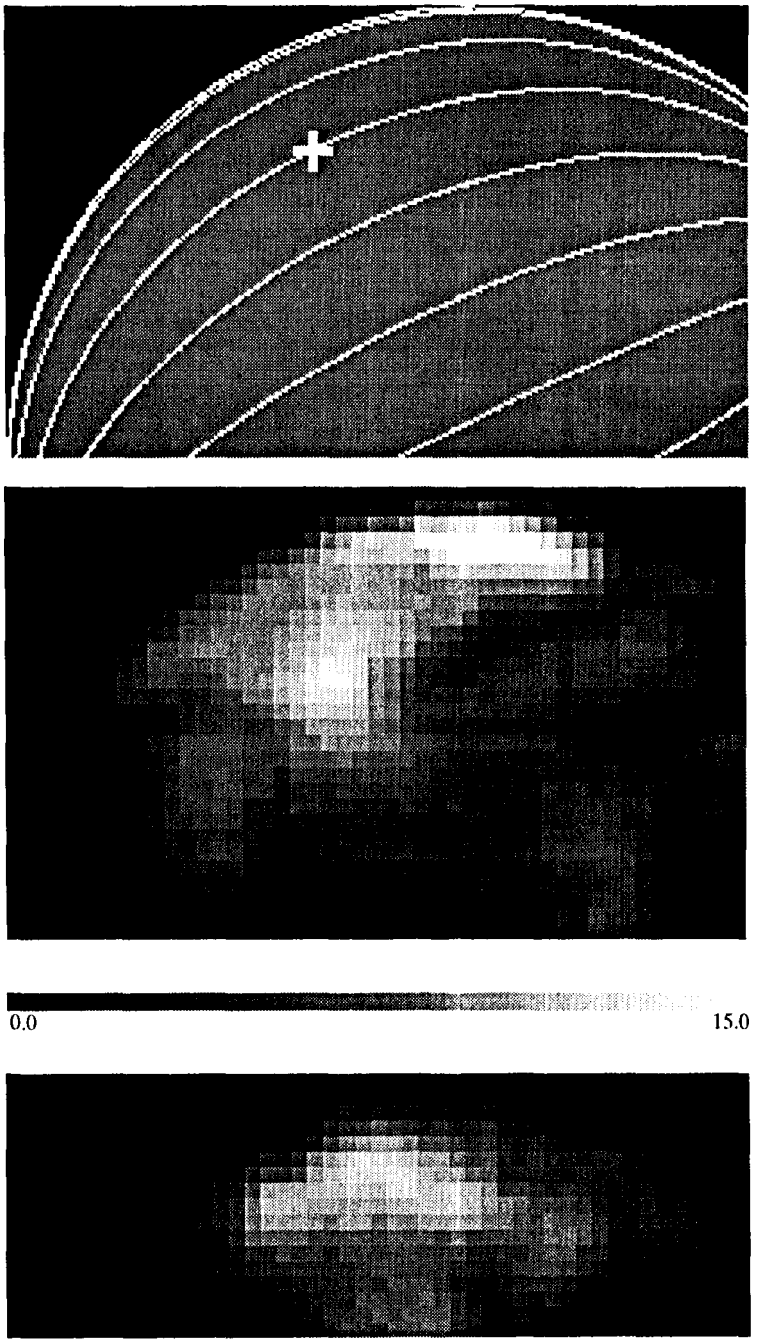

Figure 5: *AAT/IRIS observations of O_2 airglow emission on the Venus night side on 27 and 28 July, 1991. (top) Orientation of Venus, and position of the antisolar point (white cross). North is to the right, and East (on the sky) is at the top. The curved lines show local time in 1- hour increments, with local midnight running through the antisolar point, and early morning hours towards top. (middle) An O_2 airglow image from the IRIS image cube taken at 0824 UT on 27 July 1991. (bottom) An O_2 airglow image acquired 24 hours later (0824 UT 28 July). These maps show the integrated emission from the 1', Q and R branches. The scale bar shows the intensities in Mega-Rayleighs (MR). To convert these values to m W m^{-2} sr^{-1}, they should be multiplied by 0.125. Black indicates zero emission, and white shows emission exceeding 15 MR.*

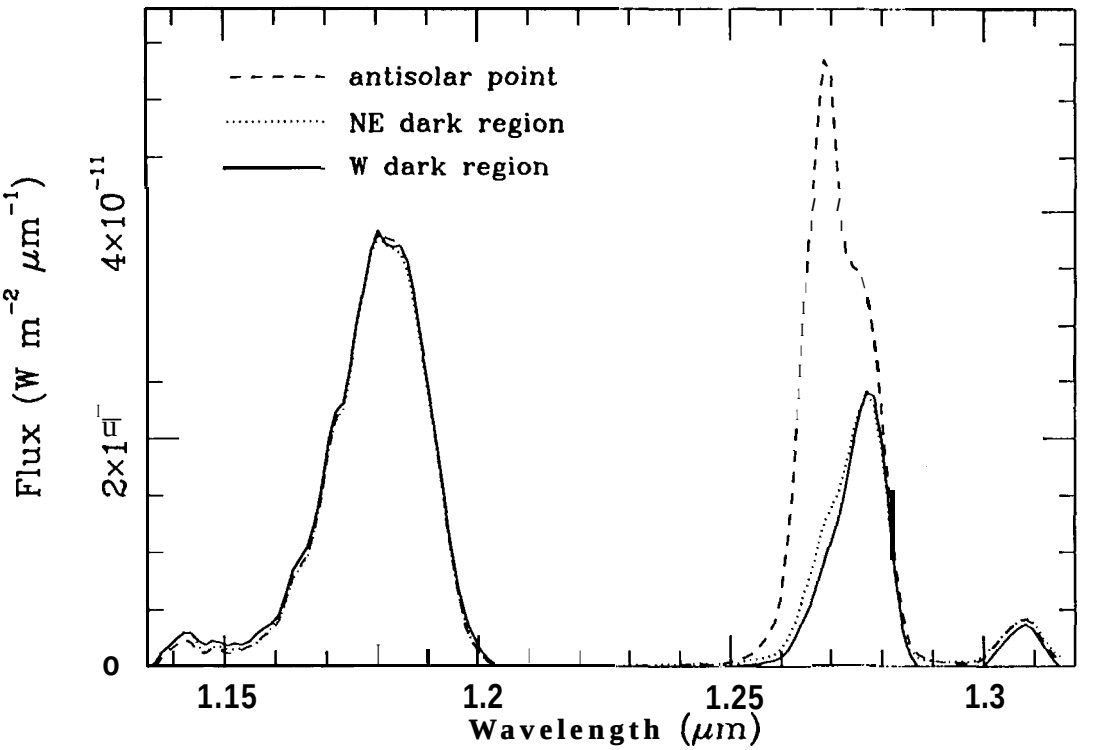

Figure 6: *Comparison of IRIS spectra from bright and dark O_2 emission regions from the image cube taken on 27 July (Figure 5). The spectrum taken at the antisolar point shows intense emission from the $0_2(a^1\Delta_g)$ Q-branch at 1.269 μm, while the spectra of the dark regions to the northeast (NE) and west (W) of the antisolar point show much less 1.269 μm emission. To facilitate comparisons, the spectrum of the western dark region was scaled by a constant, factor such that the intensity of the thermal emission peak at 1.18 μm matched that of the anti-solar point. To convert fluxes to W m^{-2} sr^{-1} μm^{-1}, ordinate should be divided by 2.52 $\times 10^{-11}$ sr pixel^{-1}*

$\sim$ *29"*. In addition, scattered light from the illuminated crescent was more of a problem since $\sim$ 41 % of the disc was illuminated. We have not yet completed the radiometric calibration of the data from this observing run, but observations taken at $\sim$19 UT on 17, 18, and 19 October showed spatial and temporal variations in 0_2 airglow that were similar to those seen in July and September. On 17 October, the emission was most intense along the equator and in a North-South band between the 1 and 3 AM meridians (Figure 8). The regions near the limb at $\sim$30S and $\sim$30N latitude brightened substantially by 18 October. The bright spot in the southern hemisphere faded substantially by 19 October, producing a southern hemisphere airglow distribution that was roughly anticorrelated with that seen the previous day.

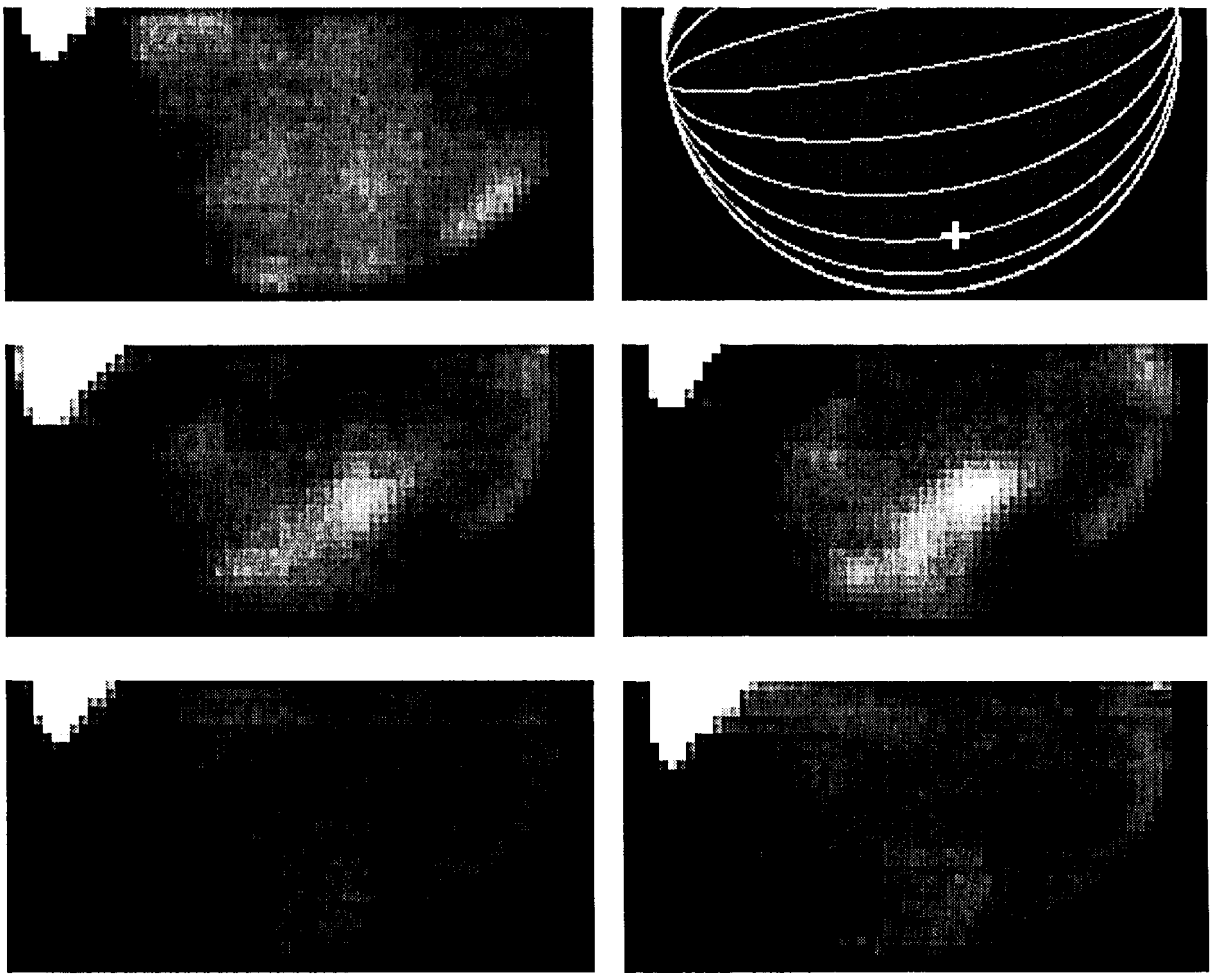

Figure 7: *AAT/IRIS observations of O_2 airglow emission* on *the Venus night side in September 1991. The upper left-hand image shows the emission observed at 0029 UT* on *17 September. The upper-right-hand image shows the orientation of Venus, and the location of the anti-solar point (white cross) North is to the right, and East (on the sky) is at the top. The two central images were taken at 2039 and 2137 UT on 19 September. The intensity of the bright feature* near *the anti-solar point increased by about 20% between these observations, but the background O_2 emission remained roughly constant. The lower two images were taken at 2039 and 2150 UT on 20 September. The* regions *of intense emission seen on the previous day had vanished.*

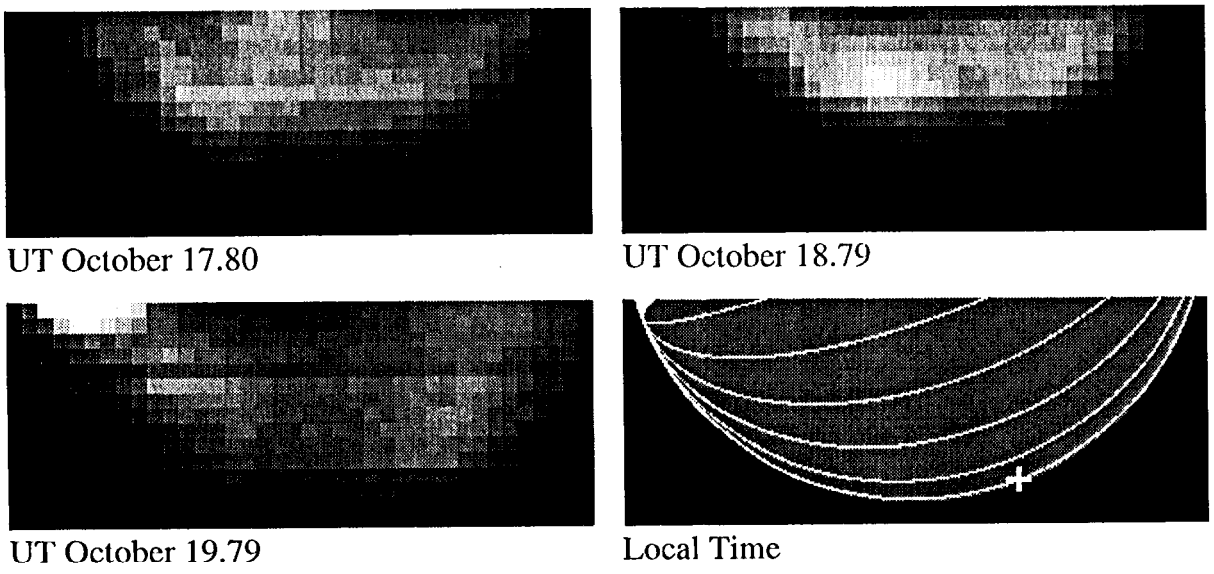

Figure 8: *AA in/IRIS observations of O_2 airglow emission on the Venus nightside limb on 17-19 October 1991. North is to the right, and East (on the sky) is at the top. The upper two images show the emission distribution at 1912 UT on 17 October and 1858 UT on 18 October. The lower left-hand image shows Venus at 1858 UT on 19 October. The lower-right-hand image shows the orientation of Venus, and the location of the anti-solar point (white cross). Local time* increases from *~midnight at the limb to the early morning hours at the top of the plot.*

2.6 October 1991 CFHT/Imaging-FTS observations:

$O_2(a^1\Delta_g)$ observations were taken with the CFHT Imaging FTS on 18 October 1991 [*Maillard and Simons* 1992; *Maillard et al., 1993], when* the angular size of the Venus disk was 29 ". This instrument provided a 24" diameter circular field of view, sampled at 0.33 "/pixel. Its spectral resolution was 1800. An 0_2 airglow image extracted from an image cube taken at 1530 UT on 18 October shows three 2" discrete bright spots (2 in the north, one in the south), distributed around a much darker spot centered at the equator. The intensity of the 0_2 airglow varied from 1.2 ± 0.12 mW $m^{-2} sr^{-1}$ in the bright spots, to 0.44 ± 0.12 mW n^{-2} $sr^{-1} \mu m^{-1}$ in the equatorial dark spot [*Maillard et al. 1993].* These results are similar to the 0_2 observations obtained $\sim$ 3.5 hours later at the AAT, but a quantitative comparison of these data sets has not yet been completed. Such a comparison would provide improved constraints on the short-term temporal variability of the airglow.

2.7 October 1991 CFHT/FTS observations:

The CFHT/FTS was used to take high-resolution (2 cm^{-1}) spectra of the 0_2 emission from selected regions of the night side on UT 23 and 24 October 1991. '1 'hc S/N of these data is not high (1 O to 20) because they were taken after sunrise during a period when the volcanic aerosols from the Mount Pinatubo eruption dramatically enhanced the intensity of the scattered sunlight. in spite of this, these data show spatial and temporal variations in the 0_2 airglow similar to those seen earlier. On 23 October, spect ra were taken at 5 N and 20 S at $\sim$ 3AM local time on Venus (Figure 9). The 0_2 airglow intensity in the spectrum taken at 5 N is comparable to that seen on July 1 (Figure 3), while the spectrum taken at 20 S was about 1.6 times as bright. On 24 October, the airglow intensity at 5 S was comparable to that seen at 5 N on the previous day.

2.8 March 1993 CFHT/Imaging-FTS observations:

The CFHT imaging FTS was used to observe the Venus nightside $O_2(a^1\Delta_g)$ airglow emission on 8 March, 1993 [*Maillard et al., 1993].* The instrument's 24" circular field of view was centered in the northern hemisphere on the night side, and covered only about half of the $\sim$ 47 " disk. On this date, the emission was subdued and relatively uniform everywhere within the aperture, with slightly brighter emission near the equator. The high-resolution spatially-resolved data provided new opportunities to derive! rotational temperature maps for the O_2 emitting layer. *Maillard et al. 1993]* derived temperatures near 190 ± 10 K from these observations.

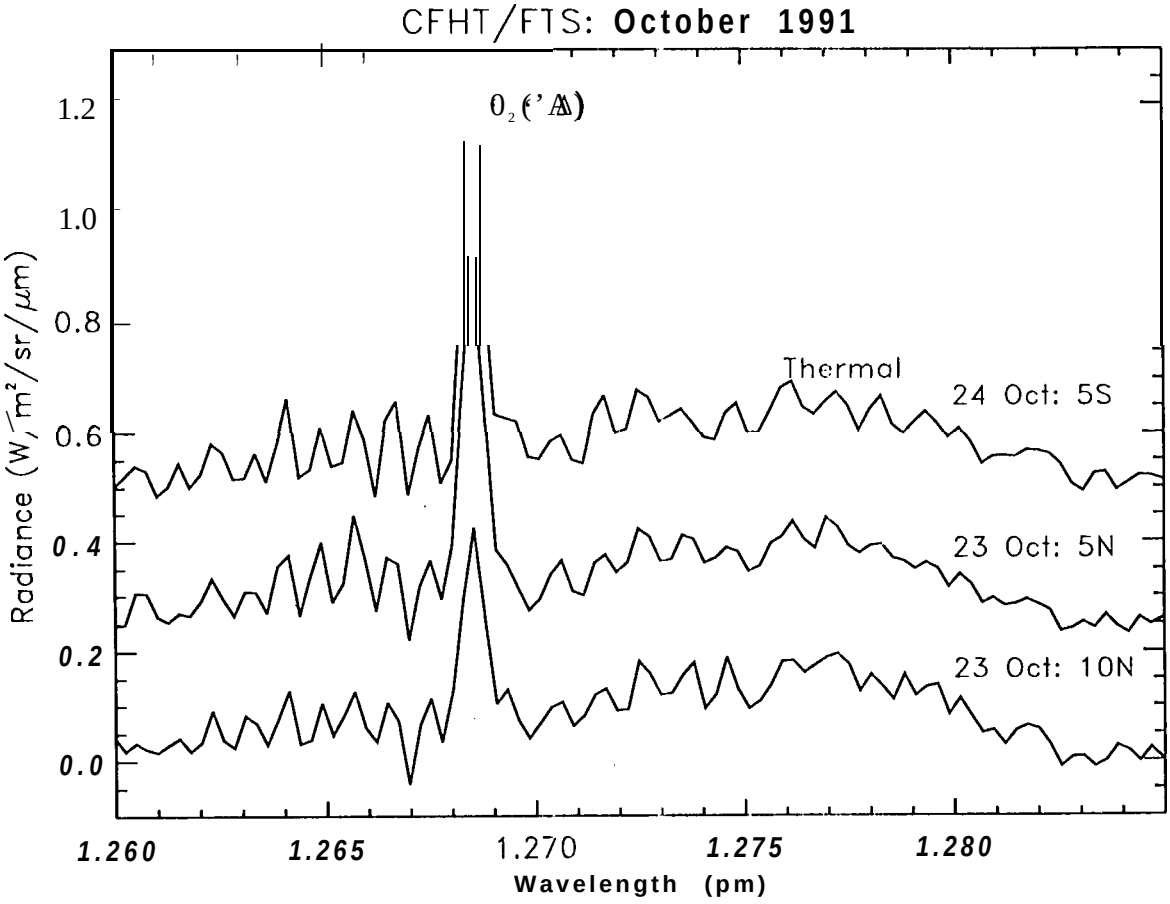

Figure 9: *CFHT/FTS spectra from 23 and 24 October, 1991. These spectra. arc offset by 0.25 W m^{-2} sr^{-1} μm^{-1} for clarity. The lower two spectra were taken by centering the 5 arcsec aperture at points near 5 N (bottom), 20 S (middle) latitude, near the 3AM meridian on 23 October. The top spectrum was taken near 5 S on 24 October.*

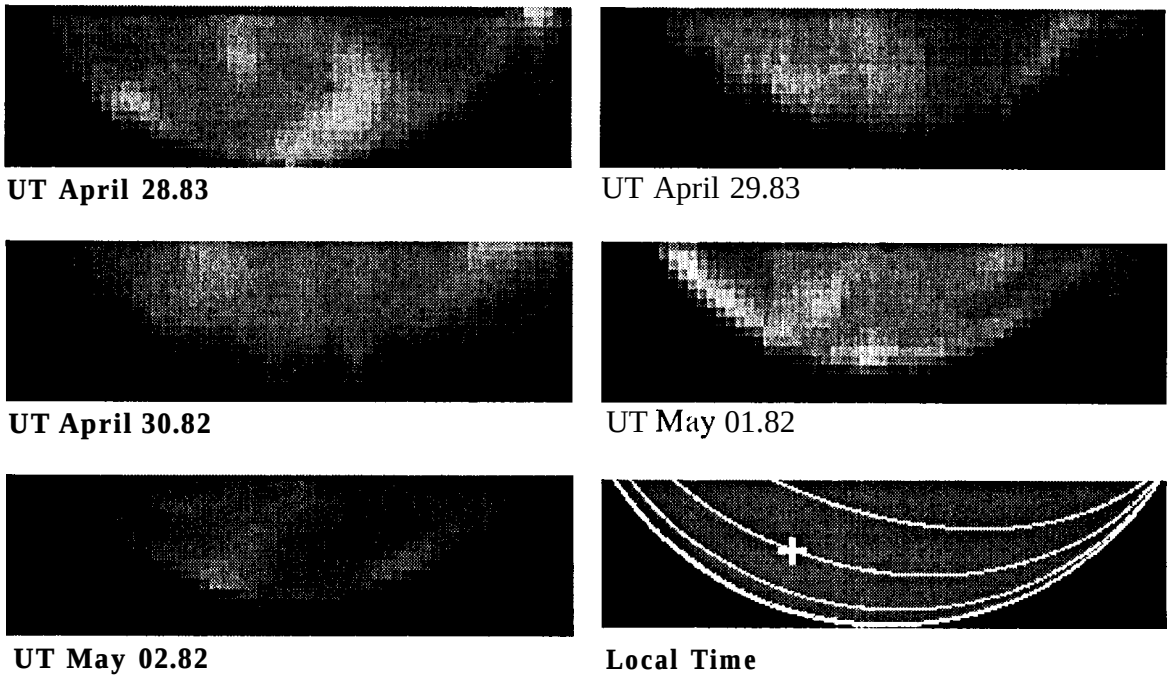

Figure 10: *AA T/IRIS observations of O_2 airglow emission from the Venus nightside limb on 28 April - 2 May 1993. North is to the right, and East (on the sky) is at the top. The lower-right-hand* image shows *the orientation of Venus, and the location of the anti-solar point (white cross), and the local time meridians.*

2.9 April 1993 AAT/IRIS observations:

One of the longest unbroken time series of 02 airglow observations was acquired with the AAT/IRIS on 28 April through 2 May 1993, when the angular sire! of Venus was $\sim$ 44" and the 10PM meridian was on the nightside limb. On 28 April, three discrete O_2 airglow emission features surrounded the anti-solar point (Figure 10). The atmospheric seeing was much worse on 29 and 30 April, but the 0_2 airglow appeared to be substantially less intense. In the 29 April images, the brightest emission was seen at low latitudes. The spatial distribution of this emission was roughly auti-correlated with that seen on the previous day. The limb had also brightened substantially at latitudes poleward of $\sim$ 45"N. On 30 April, the emission was relativel y dim everywhere on the night side, but the brightest airglow was seen just to the south of the anti-solar point. Once again, the emission near the anti-solar point was roughly anti-correlated with that seen on the previous day. On 1 May, the seeing improved, revealing intense airglow on the limb and enhanced emission over much of the night side. Discrete bright and dark airglow features were also seen between the anti-solar point and the 1AM meridian, and at $\sim$ 45°N latitude, between the 1 and 2AM meridians. On 2 May, the airglow emission from the bright limb and much of the night side had faded substantially, leaving a bright region that extended roughly cast-west from the anti-solar point to the limb.

2.10 December 1994 IRTF/CSHELL observations:

The Cryogenic Echelle Spectrograph (CSHELL) at the NASA Infrared Telescope Facility (IRTF) was used to acquire high-resolution, spatially-resolved spectra of the O_2 emission from the Venus night side on UT 2--5 and 17-24 December 1994. The 0.5 " slit was used to yield a spectral resolution of $\lambda/\Delta\lambda \sim 40000$. The spatial resolution was 0.2 "/pixel along the 30 " slit [*Greene et al.* 1993]. CSHELL observations of selected regions of the Venus night side show spatial and temporal variations in the 0_2 airglow similar to those seen earlier. Figure 11 shows a representative series of spectra of the $O_2(a^1\Delta_g)$ Q-branch acquired on UT 2 December 1994. These spectra were derived from a single 2-minute exposure, with the slit oriented East-West, across the night side, crossing the dark limb near the Venus equator. The 0_2 airglow intensity was brightest near the limb and decreased almost monotonically toward the bright morning crescent.

2.11 Summary of new observations:

The new $O_2(a^1\Delta_g)$ observations are summarized in Table 2. These data, and other observations of the Venus night side acquired at the A AT and IRTF in 1994 confirm that $O_2(a^1\Delta_g)$ airglow intensities larger than those measured by *Connes et al.* [1979] are common on the night side of Venus. They also reveal large spatial and temporal variations in this air-glow that were not anticipated from the earlier spectroscopic observati ens, which covered broad regions of the day and night sides. The brightest emission is most often seen near the limb, or in isolated regions at low latitudes, with spatial dimensions of $\sim$ 1000 km. Very dark regions, with little detectable 0_2 emission arc often seen juxtaposed with the brightest features. The intensities in the bright regions can vary by as much as 20% in one hour, and these regions often vanish entirely within one day. 1)ay-to-day variations in emission are sometimes anti-correlated, such that the brightest regions seen on one day are anomalously dark on the following day.

The airglow intensities quoted in this section have been calibrated with respect to standard stars (and with respect, to each other), but they have not been corrected for viewing-angle-dependence, reflection from the underlying clouds, self-absorption, or other artifacts of the observing geometry. These factors are derived in the following section, and applied to the observations to infer the $O_2(a^1\Delta_g)$ production rates on the Venus night side.

3 The Production of $O_2(a^1\Delta_g)$

The 0_2 airglow emission in the so-called "infrared atmospheric system" at wavelengths near 1.27 μm is produced when an 0_2 molecule in the excited $(a'\ \Delta_g)$ state spontaneously emits a photon and relaxes to its ground (0_2(X3X9)) state. This weak magnetic dipole transition has an Einstein A coefficient for spontaneous emission $\sim$ 2.58x 10^{-4} s-" [*Badger et al.* 1965;

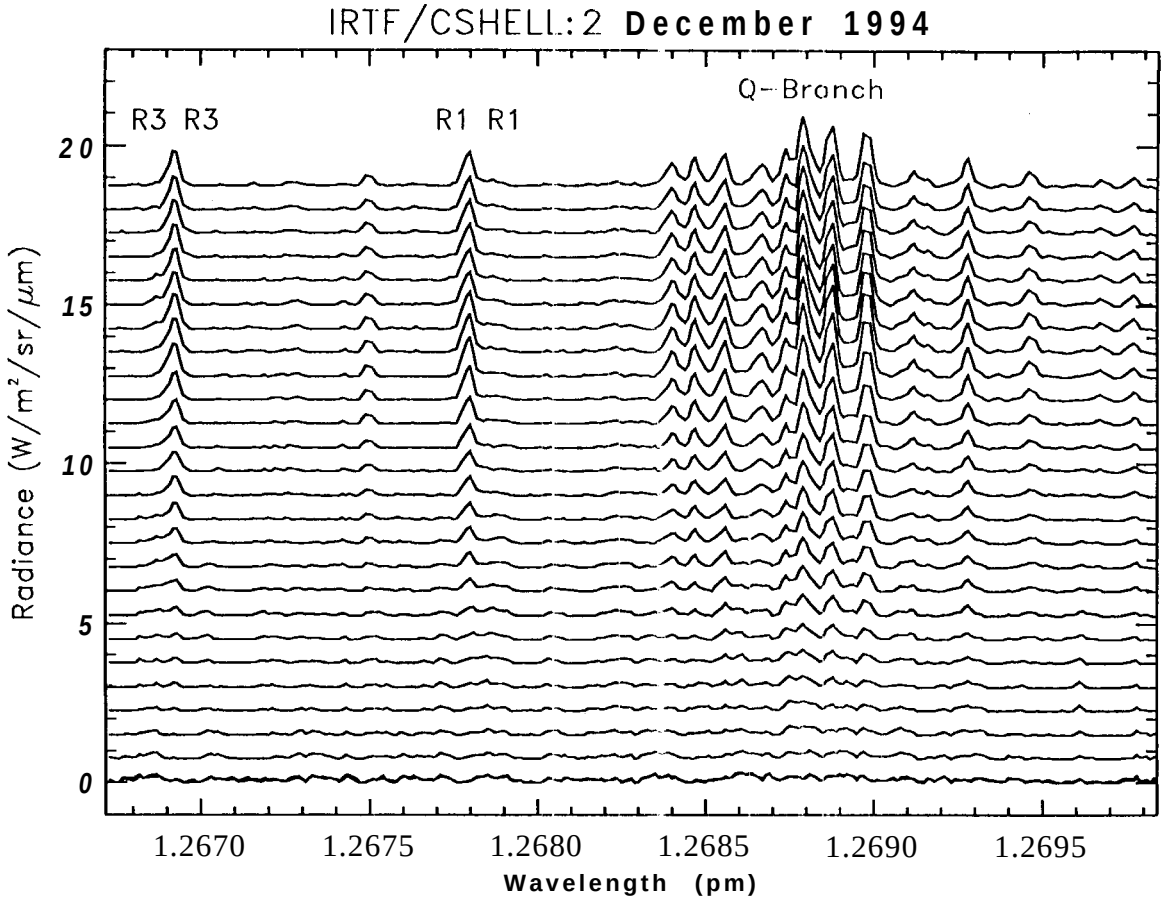

Figure 11: *IRTF/CSHELL spectra of the O_2 ($a^1\Delta_g$) Q-branch taken at 1634 UT on 2 December 1994. The CSHELL slit was oriented East- West, from the dark limb (top) to the bright* morning *terminator (bottom). Spectra were averaged* **over** *2.2 " regions along the slit and extracted at 1.0 " intervals. Integration time was 120 seconds. These spectra were collected shortly after sunrise during twilight. The 0_2 airglow intensity increases almost monotonically towards the limb.*

Table 2: Summary of Observations of $O_2(a^1\Delta_g)$ Emission

Instrument	Date (UT)	viewing angle	Intensity (MR)
AAT/FIGS	10/2/90	$< 20°$	~ 1.4
AAT/FIGS	13/2/90	$< 20°$	~ 1.4
CFHT/FTS	27/6/91	$\sim 30°$	< 1, to 1.
CFHT/FTS	1/7/91	~ 30"	8.8
AAT/IRIS	27/7/91	40°	14.2
		70°	21.5
		avg	0.94
AAT/IRIS	28/7/91	60°	8
AAT/IRIS	17/9/91	()-90°	
AAT/IRIS	19/9/91	()- 900	1.9 to 2.4
AAT/IRIS	20/9/91	()-90°	
AAT/IRIS	17/10/91	()-90°	
AAT/IRIS	18/10/91	()- 90°	
AAT/IRIS	19/10/91	()--90°	
CFHT/IFTS	18/10/91	()-90°	3.5-9.5
CFHT/FTS	23/10/91	45	8 13
CFHT/FTS	24/10/91	45	13
CFHT/IFTS	8/3/93	() 90°	
AAT/IRIS	28/4/93	()-90°	
AAT/IRIS	29/4/93	()–90°	
AAT/IRIS	30/4/93	0–90°	
AAT/IRIS	1/5/93	0-90"	
AAT/IRIS	2/5/93	()-90°	
IRTF/CSHELL	2/12/94	()- 90°	
IRTF/CSHELL	3/12/94	0-90°	
IRTF/CSHELL	4/12/94	0–90°	
IRTF/CSHELL	5/12/94	0–90°	
IRTF/CSHELL	17/12/94	()-90°	
IRTF/CSHELL	18/12/94	()-90°	
IRTF/CSHELL	19/12/94	0-90°	
IRTF/CSHELL	20/12/94	0-90°	
IRTF/CSHELL	21/12/94	0-90°	
IRTF/CSHELL	22/12/94	0-90°	
IRTF/CSHELL	23/12/94	0-90°	
IRTF/CSHELL	24/12/94	0- 90°	

Rothman 1982]. The spontaneous emission of a 1.27μm photon will therefore occur within about one hour of the formation of the excited 02 molecule. If the collision rates arc too high, however, the excited O_2 molecules can be collisionally "quenched" to their ground state, producing no airglow. The collisional quenching rates for 02 by CO_2 arc not well constrained by existing laboratory measurements, but they arc thought to be between 1 and 3 x 10-20 $cm^3 s^{-1}$ [c.f *Connes et al.* 1979; *Yung and DeMore* 1982]. These considerations suggest that the intensity of the 1.27pm O_2 airglow will be proportional to the rate of production of $0_2(a^1\Delta_g)$, but inversely proportional to the number of collisions. To satisfy these constraints, peak 0_2 emission rates should occur at altitudes between 90 and 115 km in the Venus atmosphere [Yung *and DeMore 1982; Bougher and Borucki* 1994].

3.1 Estimating 0_2 production rates from airglow intensities:

The observed intensity of the 0_2 airglow depends on several factors, including the production rates of $O_2(a^1\Delta_g)$, airmass effects associated with the viewing angle, reflection from the underlying clouds, and self-absorption by 0_2 in the atmospheres of Venus and Earth. To estimate the column-integrated O_2 production rates from these observations, we must accurate] y account for all other contributions to the observed emission. Here, wc assume that the observed intensity, I_{obs}, at sub-Earth angle, θ can be expressed in the form:

$$I_{obs}(\theta) = I(N, \theta)\, t(\tau_1, \theta) + R(N, \theta, a)\, t(\tau_2, \theta) \quad (1)$$

where, I is the intensity of the direct (upward) component of the emission from the layer, θ is the local zenith angle, $t(\tau_1, \theta)$ is the transmission along the path between the emitting layer and the observer, $R(a, 19)$ is the contribution to the observed emission reflected from the cloud tops, a *is* the cloud albedo, and $t(\tau_2, \theta)$ is the transmission along the optical path from the! base of the emitting layer, to the cloud top, and then to the observer. In principle, both 0_2 and other gases in the Venus atmosphere can produce attenuation between the emitting layer and the observer, but the results presented in the following section suggest that these sources of attenuation arc not significant, and can be neglected ($ie. t(\tau_1, \theta) = t(\tau_2, \theta) = 1$).

The direct component of the observed emission, $I(N, \theta)$, is produced by isotropic emission from excited O_2 molecules in the layer. It is therefor c a function of the number density of emitting molecules, N, the Einstein A coefficient for spontaneous emission for $0_2(a^1\Delta_g)$, and the optical pathlength, ds. Here, wc assume that the emitting layer is horizontally-infinite, (locally) plane parallel, azimuth-independent, and extends between the altitudes, z_1 and z_2. The assumption of a horizontally-infinite layer is justified for the analysis of the observations presented above, since the horizontal extent, of the emitting regions ($\sim$ 1000 km) is much larger than the vertical thickness of the layer ($\sim$ 15 km) or the distance between the emitting layer and the cloud tops ($\sim$ 25 kin). For this case, the optical path lengths through the layer scale roughly as $\sec(\theta)$, where θ is the local zenith angle. This approximation produces acceptable accuracies ($\sim$ 10% except at sub-Earth angles c1osc to the limb ($\theta > 85°$), where

it overestimates the actual path lengths. The direct contribution to the observed intensities (or '(radiances") can therefore be approximated by an expression of the form:

$$I(N, \theta) = \frac{A}{4\pi} \sec(\theta) \int_{z_1}^{z_2} N(z) dz \qquad (2)$$

where $N(z)$ is the altitude-dc~)cl~clellt O_2 number density, The division by 47r accounts for the fact that the airglow is radiated isotropically into 471 steradians. This expression indicates that airmass effects will significantly enhance the direct contribution from the O_2 emission at large sub-Earth angles, because the optical path lengths, and therefore the number of emitters along the path arc largest for those angles. To illustrate this, the direct (upward) component of the airglow at the top of the emitting layer can be expressed in the form:

$$I(N, \theta) = I_0 \; See(o) \qquad (3)$$

where I_0 is the direct contribution to the airglow intensity at normal incidence (6' = O).

The amplitude of the reflected component of the airglow, R, is somewhat less obvious, however, and different amplitudes have been derived by different observers. *Connes et al.* [1979] cites arguments presented by *Noxon et al.* [1976], adopts a cloud albedo of 0.9, and concludes that the reflected component increases the observed amplitude by a factor of $\sim$ 2.8, independent of viewing angle. Unlike *Connes, et al.*, (and this study), *Drossart et al.* [1993] assumed that the airglow seen by Galileo NIMS was spatially localized, and derived a correction factor for the reflected airglow of the fori n:

$$I_{obs}(\theta) = I(N, \theta) \; [1 + a \; \Omega \cos^2(\theta) / \pi] \qquad (4)$$

where Ω is the solid angle subtended by their observations. Evaluating this expression for their viewing angle, (θ = 46 deg; $\Omega = 1.04\pi$), assuming a cloud albedo, $a = 0.9$, they determined that the reflection from the cloud tops enhanced the emission by a factor of 1.45, about a factor of 2 smaller than that derived by *Connes et al.*

We adopted a different approach for evaluating the reflected contribution. The amplitude of the reflected radiation should depend on the intensity of the airglow illumination at the base of the emitting layer, the absorption between the cloud tops and emitting layer, and the bi-directional reflection function of the cloud top. If the airglow-emitting layer is assumed to be optically thin, (locally) plane parallel and azimuth-in dependent, as we assumed above, and if there is little attenuation between the emitting layer and the cloud tops (see next section), the intensity of the airglow incident on the cloud tops satisfies Eq. 3. If $r(\theta, \phi, \theta', \phi')$ is the angle-dependent reflection by the cloud tops, the reflected component of the airglow can be described by an expression of the form [cf. *Liou* 1980, pg 200]:

$$R(N,\theta,a) = \frac{1}{\pi}\int_0^{2\pi}\int_0^{\pi/2} I(N,\theta)\, r(\theta,\phi,\theta',\phi')\, \cos\theta'\, \sin\theta'\, d\theta'\, d\phi' \quad (5)$$

If the clouds arc Lambertian, such that $r = a$ *is* independent of angle, and the airglow intensities are described by Eq.3, this expression can be evaluated to yield

$$R(N,\theta,a) = 2\ a\ I_0 \quad (6)$$

where the factor of 2 is a consequence of the $\sec(\theta)$ dependence of the airglow intensities. If the Lambert albedo of the clouds is 0.9, this equation gives $R(N,\theta,a) = 1.810$, which is consistent with the, estimate of the reflected contribution adopted by *Connes et al.* [1979].

The clouds of Venus are not exactly Lambertian, however. To obtain improved estimates of the emission angle dependence of the reflected contribution to the observed intensities, we used a 16-stream Discrete Ordinate Model [*Stamnes et al.*, 1988], and the H_2SO_4 aerosol distributions specified in *Crisp* [1986]. We found azimuth-averaged reflectances that increased from 1.67 at $\theta = 0°$, to 1.79 at $\theta = 76°$, and then decreased to 1.73 at θ = 89° to yield an area-weighted average of the reflected contribution of $\sim$ 1.751.. These calculations show that emission angle dependence in the reflected contribution is sufficiently small that, a constant Lambert cloud albedo of, a = 0.875, can be assumed without introducing large errors. With this approximation, the observed, angle-dependent radiance emitted by O_2 can be approximated by an expression of the form:

$$I_{obs}(\theta) = I_0(\sec\theta + 2a,) \quad (7)$$

where I_0 is the radiance emitted directly from the layer at normal incidence (θ = O). This expression differs from that adopted by *Connes et al.* because it includes an emission angle-dependent direct component as well as an angle-independent contribution from the clouds. Using this formula, I_0 can can calculated directly from the measured value, I_{obs}:

$$I_0 = \text{lo}\sim,(\text{f?})/(\text{see}\ \theta + 2\text{a}) \quad (8)$$

The irradiance (flux) emitted into the upper or lower hemisphere is then given by:

$$F = \int_0^{2\pi}\int_0^{\frac{\pi}{2}} I(\theta)\cos\theta\sin\theta d\theta d\phi \quad (9)$$

Integrating this expression, wc find, $F = 2\pi I_0$. The total irradiance into both hemispheres is $4\pi I_0$, or in terms of the measured intensity, I_{obs}:

$$F = 4\pi I_{obs}/(\sec\theta + 2a) \qquad (10)$$

For historical reasons, airglow intensities are expressed in Rayleighs (or Mega Rayleighs, MR), where 1 Rayleigh=10^6 photons $cm^{-2}s^{-1}$ into 4π steradians. Wavelength dependent irradiances can be converted to Rayleighs by dividing by the energy of 10^6 photons, $(10^6\, h\, c\lambda^{-1})$, and then integrating over the spectral range. For example, if F is expressed in W m^{-2} pm-l, the flux in Rayleighs is given by

$$F_R = \frac{10^{-6}}{h\,c}\,\frac{10^{-6}\,\mathrm{m}}{\mu\mathrm{m}}\,\frac{10^{-4}\mathrm{m}^2}{\mathrm{cm}^2}\int_{\lambda_1}^{\lambda_2} F\,\lambda(\mu m)\,d\lambda \qquad (11)$$

where Planck's constant, h=6.626 x 10-"34 Js, and the speed of light, c=2.998 x 108 m S--l are expressed in S1 units. If **F** is the spectrally-integrated flux in a narrow spectral region near 1.269pm, this expression can be simplified to:

$$F_R = \mathbf{6.39}\ \times 10^8\ \mathbf{F} \qquad (12)$$

On July 1, 1991, the spectrally-integrated O_2 airglow intensity observed at the CFHT was approximately I_{obs} = 1.1 mW m^{-2} sr^{-1}. The emission angle of this spectrum is not known precisely, but if we assume a sub-Earth angle near 30°, the effective emission rate by the layer is 3 x 10^{16} photons m^{-2} s"'", or 3 MR. The bright (2.7 ± 0.2 mW $m^{-2}sr^{-1}$) air-glow emission observed near the limb on 27 July 1991 with AAT/IRIS was centered at ~ 70° sub-earth angle. Correcting for the emission angle effects and the reflection from the underlying clouds, we find an emission rate 5.8 ± 0.4 MR (where the error bars include uncertainties in the emission angle as well as those for radiance). For comparison) the somewhat less intense (1.8 ± 0.2 mW m^{-2} sr^{-1}) emission near the anti-solar point in that image was at a sub-earth angle of ~ 40°. Correcting for air mass effects, we find an emission rate of ~ 5.2 MR. The hemispheric average emission rate for the night side (excluding regions very close to the limb or the bright crescent) is 1.08 ± 0.2 MR. This result is similar to, but somewhat smaller than the nightside emission rate derived by *Connes et al.* [1979], It is important to note, however, that even though they used a similar factor to correct for cloud reflection, their analysis ignored the emission angle dependence in the direct emission, which was included here.

3.2 The absorption of $O_2(a^1\Delta_g)$ airglow in the Venus atmosphere:

The physics of the $O_2(a^1\Delta_g)$ emission also has important implications for the role of self-absorption by O_2 in the atmosphere of Venus. In most atmospheric radiative transfer modeling applications, the relationship between absorption and extinction by gases is governed by

Kirchoff's Law, since both processes are governed by the Einstein coefficient for stimulated emission, B. This is not the case for the O_2 airglow, which is a consequence of a different physical process - spent aneous emission. The relationship between (stimulated) absorption and airglow emission by O_2 is therefore determined by the relative values of these Einstein coefficients. *Rothman [1982]* relates these factors and expresses the absorption line strength, S, iu terms of the A coefficient as follows:

$$S(T) = \frac{A_{00}\nu}{8\pi\nu^3 c}\frac{S_J^N}{Q(T)} exp(-hcE''/kT [1 - exp(-hc\nu''/kT)] \quad (13)$$

In this expression, $A_{oo} = 2.58$ x 10-"4 s-1 is the Einstein A coefficient for spontaneous emission for the $O_2(a^1\Delta_g)$ band, ν is the wavenumber of the transition, (cm-1), E'' is the lower- state energy (cm^{-1}), h=6.626 x 10-27 erg s, is Planck's constant, k=1.38 x 10^{-16} ergs K^{-1} is Boltzmann's constant, and c=2.998 x 10^{10} cm s^{-1} is the speed of light (all in *cgs* units). The quantity, S_J^N, is the Hönl- London factor, which typically has values of order unity. This expression yields strengths of ~ 5 x 10^{-26} cm-1 $molecule^{-1}$ cn^{-2} for the strongest lines. The maximum O_2 optical depths are given by:

$$\tau(O_2) = \int_{z_1}^{\infty} S(T) f(\nu - \nu_0, T) N(z) dz \quad (14)$$

were $f(\nu - V_o, T)$ is the line-shape function, and the integral extends from the cloud tops, z_1=65km, to ∞. If the 0_2 mixing ratios above the cloud tops are close to 10-7, [*Trauger and Lunine* 1983], the mesospheric 0_2 column densities are of order 2 x 1017. For these 0_2 abundances, our line-by-line calculations indicate mesospheric 02 optical depths < 10^{-6} in the cores of the strongest lines. These calculations show that in spite of the high intensities of the 0_2 airglow, the self absorption by 0_2 is completely negligible.

CO_2 is the only other gas that absorbs significantly in the vicinity of the $0_2(a^1\Delta_g)$ band. We found that the normal-incidence, CO_2 line-core, optical depths are no larger than 0.01 within the Q-branch of the $O_2(a^1\Delta_g)$ band. The CO_2 line-core optical depths increase to about 0.1 in the R-branch of the $O_2(a^1\Delta_g)$ band, but both the 0_2 and CO_2 lines are narrow, and few strong $C0_2$ lines fall at the same wavelength as the 0_2 lines. $C0_2$ is therefore not a major sour-ce of extinction for the 0_2 air-glow.

4 Discussion

4.1 Chemical modeling of $O_2(a' \Delta_g)$ production rates:

There have been several attempts to simulate the airglow emission with l-dimensional, steady state, photochemical models [*Parisot and Moreels 1980; Yung and DeMore 1982;*

Krasnopol'sky and Parshev 1983]. In these models, the $O_2(a^1\Delta_g)$ is produced primarily by the recombination of atomic oxygen that is created by the photodissociation of $C0_2$[Connes *et* al. 1979], or $S0_2$[*Leu et al. 1987],* or the photolysis of O_3[*Parisot and Moreels 1980] on* the day side of Venus. This atomic oxygen can recombine on the day side where it is produced, or be transported from the day side to the night side by the global circulation. The 3-body and catalytic recombination reactions listed in TaMc 1 are sufficiently exothermic to yield 0_2 in the excited $(a^1\Delta_g)$ state (E = 0.98 eV), but only the 3-body reaction (O + O + M $\rightarrow O_2(a^1\Delta_g)$ + M), produces 02 with enough excess energy to produce an optical photon (5 eV).

However, unrealistically high $O_2(a^1\Delta_g)$ production rates are required to produce the observed airglow emission rates (> 1 MR). The CO_2 photodissociation rates are known to be near 8 x 10^{12} e n^{-2}s- ^{1}[*Leu et al. 1987].* This suggests maximum O O recombination near 4 x 10^{12} cm^{-2} S-1. If the quantum yields of the $0_2(a^1\Delta_g)$ production reactions in Table 1 were close to 100%, and collisional quenching were completely negligible, these reactions would produce globally-averaged 0_2 airglow intensities near 4 MR, and we could easily explain the observed intensities. These assumptions are unrealistic, however. Recent laboratory measurements indicate typical quantum yields of $\sim$ 4% for these reactions [*Leu et al.* 1987]. With these low quantum yields, the maximum global-average 0_2 airglow intensities should be closer to 0.16 MR. The presence of collisional quenching will reduce this even further.

Airglow intensities greater than 1 MR therefore imply additional sources of atomic oxygen, or reactions that produce $O_2(a^1\Delta_g)$ emission without O- O recombination reactions. For example, the photolysis of SO_2 could provide an additional source of atomic oxygen [*Leu et al. 1987].* $S0_2$ mixing ratios like those measured since 1979 (0.1 ppm) provide little additional atomic oxygen, but a hundred-times enhancement in the mesospheric $S0_2$ abundance might produce enough atomic oxygen to account for the airglow seen by *Connes et al.* [1979]. *Leu et al. [1* 987] therefore speculate that the high 0_2 airglow intensities measured in 1975 may have been associated with a massive injection of SO_2 into the upper mesosphere (by a volcano or some other process). This hypothesis could not be evaluated directly because the first mesospheric $S0_2$ measurements were acquired about 4 years after the 02 airglow observations were taken. However, this mechanism cannot explain the more recent observations of bright O_2 airglow, which were taken during a period when the SO_2 mixing ratios were $\sim$ 0.1 ppm at the cloud tops, with a scale height of $\sim$ 3 km [*Na et al.* 1990; *1994].* No additional mesospheric sources of atomic oxygen have been identified.

Leu *et al.* also proposed a reaction that uses chlorine as a catalyst to produce $O_2(a^1\Delta_g)$ without creating any new O- 0 bonds. Their scheme includes the following steps:

$$\begin{aligned} Cl + 0_2 + M &\rightarrow ClO_2 + M \\ Cl + ClO_2 &\rightarrow C1_2 + O_2(a^1\Delta_g) \\ Cl_2 + h\nu &\rightarrow 2Cl \\ \hline net: \quad O_2 &\rightarrow O_2(a^1\Delta_g) \end{aligned}$$

When the best available quantum yields were used for these reactions in the model described

by *Yung and Demore* [1 982], this reaction produces airglow intensities of only 0.2 MR, well short of that needed to account for the observed intensities. One asset of this scheme is that even though the chlorine! must be recycled on the day side, the $O_2(a^1\Delta_g)$ can be produced on either the day or the night side. This attribute is essential for any chemical mechanism that attempts to account for the nightside emission, because once an O_2 molecule is created in the excited $(a^1\Delta_g)$ state, it will emit a photon and return to its ground state within $\sim$1 hour. It is therefore unlikely that molecules can be transported from the day to the night side on this time scale.

The new observations of $O_2(a^1\Delta_g)$ emission from the Venus night side cannot solve the apparent O_2 budget deficit, but they contain valuable clues to the relevant chemical mechanisms. For example, they show that the brightest airglow is usually confined to isolated regions, with spatial dimensions of order 1000 km. They also i ndicate that the brightest regions can vary by as much as 20%0 in periods as short as 1 hour, and that these regions have lifetimes of less than one day. 1 lowever, this transience does not solve the budget problem because the average nightside emission rates rarely fall below $\sim$0.5 MR, even when no discrete bright spots are present. It dots suggest that the processes producing $O_2(a^1 A_g)$ involve a chemical constituent or physical condition that varies significantly with time. The observed temporal and spatial variations also suggest that I-dimensional, steady state, chemical models might not be adequate for exploring the mechanisms that produce this airglow.

4.2 Spatial variations in the nightside $O_2(a^1\Delta_g)$ airglow:

In spite of the fact that existing chemical models cannot yet account for the observed intensities of the 0_2 emission on the night side of Venus, recent investigations of thermospheric dynamics are providing insight into the observed spatial and temporal variations in this airglow. Early modeling studies suggested that the circulation above $\sim$90 km was dominated by a subsolar to antisolar (SSAS) flow, with upwelling over the subsolar point, rapid flow across the terminator, and subsidence at the anti--solar point [*Dickinson and Ridley 1975; Dickinson and Ridley* 1977]. This circulation could potentially transport mom atomic oxygen from the day side to the night side 'than a quasi-horizontal circulation because the upwelling branch of this cell transports the atomic oxygen produced in the upper mesosphere and lower thermosphere to higher altitudes (lower pressures) where the recombination rates arc much lower. The downward flow near the anti-solar point would then carry atomic oxygen back through the mesopause, where the recombination rates, and $0_2(a^1\Delta_g)$ production rates are larger. These early models therefore offer at least a partial explanation for the large O_2 airglow intensities observed on the Venus night side, but they provide little insight into the observed spatial and temporal variability in this emission. This variability suggests that the thermospheric circulation and 0_2 transport may be substantially more complicated.

Recent efforts to analyze Pioneer Venus observations of thermospheric densities [*Brinton et al.* 1980] and () and NO airglow at ultraviolet wavelengths [*Stewart et al. 1980; Alexander 1992; Alexander et al. 1993]* also indicate a somewhat more complicated situation. Simulations of these phenomena with the Venus Thermospheric General Circulation Model

(VTGCM)[*Bougher et* al. 1990; *Fox and Bougher 1991; Bougher and Borucki 1994]* indicate that the SSAS flow is superimposed on an east- west (zonal) super- rotation. Recent ground- based Doppler measurements of thermospheric wind speeds at infrared [Goldstein *et al.* 1991], and millimeter wavelengths [*Shah et al.* 1991; *Lellouch et al.* 1994] wavelengths appear to support this basic picture, but these observations disagree on the relative amplitudes of the SSAS and zonal flows. Infrared heterodyne measurements of Doppler shifts in CO_2 lines indicate cross-terminator SSAS velocities of ~ 120 m s^{-1}, and zonal velocities of 25 m s--l at altitudes near 110 km. Shah *et al. [1991]* measured Doppler shifts in the 2.66 mm CO line in 1988 and found larger zonal winds (~ 85 m s^{-1}) and a weaker SSAS flow at altitudes near 100 km. In contrast, CO observations taken in 1991 by *Lellouch et al.* [1994] indicate SSAS and zonal velocities with similar amplitudes (40+ 15 m S-l at 95 km, increasing to 90 ± 15 m s^{-1} at 105 km). These differences might reflect, systematic errors in the observations, but there is increasing evidence that they indicate real spatial and/or temporal variations in the thermospheric circulation.

The mechanisms that might drive the zonal component of the thermospheric circulation were not immediately obvious, but a recent analysis of PV OUVS observations of the 0.1304 μm oxygen airglow *[Alexander 1992; Alexander et al.* 1993] indicates that this super- rotation may be maintained by zonal momentum transports associated with vertically - propagating gravity waves that arc generated within the clouds. These waves have predominantly westward phase velocities and phase speeds that are similar to the cloud-level winds ($\sim$ 100 m S-l). Their amplitudes increase as they propagate upward through the mesosphere, until they reach the lower thermosphere, where they break, and deposit their (westward) momentum to drive the thermospheric super--rotation. This model predicts strong local-time variations in the effects of this wave momentum forcing on the SSA S flow, since the westward propagating waves will decelerate the SSAS flow in the morning hemisphere, and accelerate it in the afternoon hemisphere [*Alexander et al. 1993].* This wave forcing mechanism could also produce large temporal variations in the thermospheric circulation if there were changes in the cloud- top wave production, or the mesospheric thermal structure and dynamics. This transience could be caused by temporal variations in the cloud-top forcing of these gravity waves, or changes in the altitude at which they break. If these waves are generated by convective turbulence associated with heating of the cloud-top UV absorber [Crisp 1986, 1989], the wave amplitudes could change with a 4-5 day period, as the "Y"- shaped UV albedo feature rotates around the planet. These changes might alter the atomic oxygen transport from the day to the night side of the planet, contributing to the observed temporal variations in the O_2 airglow.

Bougher and Borucki [1994] used the VTGCM to illustrate the impact of these processes on the intensity and spatial distribution of nightside $O_2(a^1\Delta_g)$ airglow emission. Their nominal case, which assumed weak zonal winds in the lower mesosphere, produced 02 airglow intensities that varied by a factor of 8 across the night side, with peak intensities (0.54MR) centered at the equator at 1AM local time. When the westward zonal wind speeds were increased to > 50 m s^{-1} in the lower thermosphere, gradients in the 0_2 intensities on the night side were smeared out, and the local time of peak emission moved to 4- 5AM.

To simulate the effects of variations in the gravity wave forcing mechanism mentioned above,

they also varied the Rayleigh friction at thermospheric levels. They found that a 50% decrease in this drag produced a 50-230 m s^{-1} increase in the cross-terminator velocities. This enhanced the atomic oxygen transport and increased the $O_2(a^1\Delta_g)$ airglow intensities by $\sim$ 30'%. These simulations confirm that variations in the zonal component of the transport, and the strength of the gravity wave momentum forcing of the super- rotation, could produce much of the observed variability in the airglow.

These results provide additional insight into the mechanisms that produce the observed airglow variations, but they still offer an incomplete explanation of the observed spatial and temporal variability. In particular, these steady stat c models do not explain why the O_2 airglow production changes so rapidly, or why the brightest regions seen onc day arc often the darkest on the next day. Wc attempt to address t hcsc issues in the following section.

4.3 Temporal variations in the nightside $0_2(a^1\Delta_g)$ airglow:

Ncw observations of $O_2(a^1\Delta_g)$ airglow from the Venus night side confirm that emission rates exceeding 1 MR arc common. They also reveal dramatic spatial and temporal variations in this airglow that had not been anticipated from earlier spectroscopic observations. If this $0_2(a^1\Delta_g)$ airglow is produced primarily by the recombination of oxygen atoms that arc produced on the day side of Venus, as existing chemical models predict, the nightside airglow intensity can be modulated by: *(i)* changing the atomic oxygen production or recombination rates on the day side, *(ii)* altering the atomic oxygen transport from the day side to the night side *(iii)* varying the recombination rates of O atoms 011 the night side or *(iv)* changing the relative importance of radiative and collisional de excitation of the $O_2(a^1\Delta_g)$ molecules on the night side.

If the atomic oxygen production rates on the day side of Venus are dominated by the UV photolysis of CO_2, these rates should not change on hourly or daily timescales, because the intensity of UV radiation and abundance of $C0_2$ should remain constant on these timescales. Short-term variations in the abundance of other trace species on the day side, like $S0_2$, could produce changes in the atomic oxygen production rates, but no significant sources have been identified.

The nightside O-atom supply can also be modulated by changing the atomic oxygen recombination rates on the day side. These rates could be changed either by altering the concentration of catalytic species (Cl_x, HO_x), or by changing the vertical mixing rates between the upper mesosphere and the thermosphere. The formation of O- O bonds by three- body recombination should not vary significantly with time, because the rate of this reaction depends only on the local atmospheric bulk density. The rates of day side 0_2 recombination by the catalytic reactions listed in Table 1 could vary substantially if there were large temporal variations in the mesospheric concentrations of Cl, ClO, or HO_2.

IIay-side O_2 recombination rates arc also affected by the vertical transport rates because recombination rates arc slower at higher altitudes. If the vertical diffusion rates arc small, and the circulation is dominated by upward advective transport on the day side, a larger

fraction of the oxygen that is produced at mesospheric levels will be transported to high altitudes. If the dayside vertical transport is dominated by eddy diffusion, the net transport will depend on the vertical gradient in the atomic oxygen concentration (which is thought to be positive, such that the O concentration increases with altitude [*Yung and Demore* 1982], and much less mesospheric atomic oxygen will be transported to the thermosphere before it recombines. *Alexander et al. [1993]* used the VTGCM to illustrate this mechanism. Their calculations show that the thermospheric O abundance decreases by as much as 40% when the vertical eddy diffusion coefficients are increased by a factor of 8. The thermospheric O abundance increases by 25- 30% when the diffusion coefficients are set to zero. These results suggest that temporal variations in the eddy diffusion coefficients could contribute significantly to thermospheric atomic oxygen supply and the brightness of the nightside O_2 airglow.

Bougher and Borucki [1994] show that the gravity- wave mechanism in-ol)oscd by *A lexander* [1992] can alter the nightside atomic oxygen supply by modulating, the intensity of the flow across the terminator. in principle, this mechanism could also produce significant temporal variations in the vertical eddy diffusion coefficients in the lower thermosphere if the altitudes at which the waves break varies with time. By analogy with the Quasi- Biennial oscillation (QBO) in the Earth's tropical stratosphere, the breaking gravity waves could transport enough westward momentum to the thermosphere to create a critical layer. Subsequent waves would then be absorbed at or below this critical layer, forcing the altitude of this layer to propagate downward with time. If this mechanism operates over the (90 125km) range, it could produce significant temporal variations in the eddy diffusion near the mesopause, and the atomic oxygen supply in the thermosphere.

The processes described above affect the supply of atomic oxygen to the thermosphere. Once there, several factors can influence the spatial and temporal distribution of the O atoms and their recombination on the night side to form 0_2 airglow. Processes that affect the steady state transport from the day to the night side are discussed in the previous section. Here we will focus on the subsiding branch of the circulation.

The observed variability of the nightside 0_2 airglow might be associated with one of several chemical processes that produce $O_2(a^1\Delta_g)$. For example, these variations could be associated with time-varying spatial structure in the concentrations of trace constituents needed for the gas-phase recombination reactions. Alternatively, the observed variability could be a consequence of chemical processes that have not yet been explored, including heterogeneous chemical reactions, involving H_2SO_4 aerosols, meteor ic debris or other agents (Y. L. Yung, personal communication, 1995). In the Earth's upper atmosphere, the abundance of aerosols, ices, and meteoric debris as catalytic sites for heterogeneous reactions is highly variable. If similar conditions exist on Venus, these variations could explain some of the observed structure in the airglow (e.g. Huestis and Slanger [1993] identified a long, narrow feature in the NO airglow observed by PVO and suggested it might have been a meteor track). These possibilities cannot be ruled out, but very little is known about the rates of such heterogeneous reactions, thus, their ability to in-oducc the observed intense airglow emissions is unknown.

The presence of discrete bright patches of O_2 emission suggests that the downward transport is often spatially confined. Isolated regions of enhanced subsidence and air-glow emission have been adequately simulated in steady state VTGCM simulations [*Bougher and Borucki, 1994]* but the observed temporal variability has not yet been explained. In particular, these models do not explain the presence of very dark regions juxtaposed with the brightest regions, or the occasional appearance of airglow patterns that are roughly anticorrelated with those seen on the previous day. These observations suggest that the O_2 airglow is being switched off, not simply dispersed across the night side by increasing 10W-1CVC1 zonal winds or other dynamical processes. Mechanisms that dramatically alter the day-side supply of thermospheric O atoms might lead to large-scale reductions in the airglow brightness, but these processes are not likely to produce sharply defined features in the nightside airglow. Such features are probably produced by local chemical or dynamical processes on the night side.

One possibility is that the rapid subsidence associated with bright airglow emission regions may produce adiabatic (compressional) heating. If the compressional heating rates exceed the radiative cooling rates, this process will increase the local static stability and interfere' with the subsidence. This could cause a rapid reduction in the emission, producing a dark region. The subsidence will then shift to another region of the planet until the heated region recovers. Radiative relaxation times at 90-- 100km are about 1day [Crisp 1989], comparable to the time scales of the observed airglow variability.

in principle, it should be possible to test this hypothesis by monitoring the temperatures of bright, airglow emitting regions. The pressures at these altitudes are sufficiently high that the $O_2(a^1\Delta_g)$ should be in rotational local thermodynamic equilibrium. The rotational temperature of the 0_2 molecules should therefore provide a good measure of the ambient gas temperature. The rotational temperature of the $O_2(a^1\Delta_g)$ can be obtained by measuring the relative strengths of the lines in the far wings of the P and 1 ℓ branches relative to the Q-branch emission. We attempted to create spatially-resolved temperature maps using the AAT/IRIS observations from July 1991. This analysis indicated that the bright spot near the anti-solar point may have been somewhat warmer than the surrounding atmosphere, but the S/N was not sufficient to provide a definitive test of this mechanism [*Meadows 1994].* High-resolution, spatially-resolved spectra like those recently collected with the CFHT Imaging FTS and the IRTF/CSHELL are currently being analyzed to provide improved estimates of the correlation between airglow intensity and temperature. These results will be reported in a subsequent paper.

5 Conclusions

Ground based imaging and spectroscopic observations of 1.269 μm 02 $(a^1\Delta_g)$ airglow emission, taken between 1990 and 1994, show disk- averaged airglow intensities that are in excellent agreement with those reported by Connes *et al.* [1979]. These new observations also show dramatic spatial and temporal variations in the airglow from the night side of Venus, with observed intensities varying from 1 to $\sim$ 20 MR. The brightest regions vary by more than 20% on time scales of one hour, and can disappear entirely in less than one day. In

addition, there is some evidence for an anti-correlation in the airglow pattern observed on consecutive days. Sharply-defined dark regions that show almost no airglow emission are often found adj acent to the brightest regions.

To obtain accurate estimates of the emission rates from the observed airglow intensities, we derived factors to account for emission angle effects and the reflection from the underlying clouds, We also found that the self absorption by O_2 was completely negligible, and that CO_2 is not a major source of extinction for the O_2 airglow. Applying these correction factors to our observations, we confirm that the observed airglow intensities correspond to nightside-averaged emission rates exceeding 1 MR. These emission rates are far in excess of those predicted by existing 1-dimensional steady state chemical models. Recent efforts to model the dynamics of the Venus then-mosphere have provided some clues to the observed spatial variations in the 0_2 airglow, but provide little direct insight into the temporal variability of this emission, or the frequent juxtaposition of sharply-defined bright and dark regions. We have proposed that these phenomena may be a consequence of localized heating, produced in the subsiding branch of the SSAS circulation. This hypothesis will be tested by producing spatially resolved rotational temperature maps of the 0_2 airglow emission and searching for correlations between the observed airglow intensities and temperatures.

Acknowledgements

This paper is dedicated to the memory of our collaborator Dr David A. Allen (1946- 1994). Part of this work was conducted at the Jet l'repulsion Laboratory/California Institute of Technology. DC grateful] y acknowledges support from the NASA Planetary Atmospheres Program and the NASA Venus Data Analysis Program. This work represents partial fulfillment of the requirements for VSM'S PhD degree at the University of Sydney, Australia. VSM was supported in part by an Australian Postgraduate 1 tesearch Award and also acknowledges generous financial support from the Australian Federation of University Women-South Australia. We also acknowledge generous support from the time allocation committees of the Anglo-Australian Observatory, Canada-France Hawaii Telescope (operated by the National Research Council of Canada, the Centre National de la Recherche Scientifique de France, and the University of Hawaii), and NASA infrared Telescope Facility.

References

Alexander, M. J. A mechanism for the venus thermospheric superrotation. *Geophys. Res. Lett.*, 19:2207, 1992.

Alexander, M. J., A. 1. l?. Stewart, and S. C. Solomon. Local time asymmetries in the Venus thermosphere. *J. Geophys. Res.*, 98(E6):10,849 10,871, 1993.

Allen, D. A. IAU Circ., 1990. 4962.

Allen, D. A., J. R. Barton, M. G. Burton, H. Davies, T. J. Farrell, P. R. Gillingham, A. F. Lankshear, 1'. L. Lindner, D. J. Mayfield, V. S. Meadows, G. E. Schafer, K. Shortridge, J. O. Spyromilio, J. amd Straede, L. G. Waller, and D. I,. Whittard. IRIS: an infrared imager and spectrometer for the Anglo-Australian Telescope. *Proc. Astron. Sot. Aust.*, 10:298-309, 1993.

Allen, D. A., D. Crisp, and V. S. Meadows. Variable oxygen airglow on Venus as a probe of atmospheric dynamics. *Nature,* 359:516-518, 1992.

Badger, R. M., A. C. Wright, and R. F. Whitlock. *J. Chem. Phys.*, 43:4345, 1965.

Barker, E. S. Detection of SO_2 in the UV spectrum of Venus. *Geophys. Res. Lett. , 6:117-120,* 1979.

Bougher, S. W., and W. J. Borucki. Venus O_2 and IR nightglow: Implications for lower thermosphere dynamics and chemistry. *J. Geophys. Res.*, 99(E2) :37593776, 1994.

Brinton, H. C., H. A. Taylor, Jr., H. B. Niemann, H. G. Mayr, A. F. Nagy, T. E. Cravens, and D. F. Strobel. Venus nighttime hydrogen bulge. *Geophys. Res. Lett.*, 7:865-868, 1980.

Connes, P., J. F. Noxon, W. A. Traub, and N. P. Carleton. $O_2(^1\Delta)$ emission in the day and night airglow of Venus. *Ap. J. (Letters),* 233:L29 L32, 1979.

Crisp, D. Radiative forcing of the Venus mesosphere. I. Solar fluxes and heating rates. *Icarus*, 67:484-514, 1986.

Crisp, D. Radiative forcing of the Venus mesosphere. 11. Thermal fluxes, cooling rates, and radiative equilibrium temperatures. *Icarus*, 77:391-413, 1989.

Crisp, D., D. A. Allen, D. H. Grinspoon, and J. B. Pollack. The dark side of Venus: Near-infrared images and spectra from the Anglo-Australian Observatory. *Science*, 253:1263-1266, 1991.

Crisp, D., S. McMuldroch, S. K. Stephens, W. M. Sinton, B. Ragent, K. W. Hodapp, R. G. Probst, L. R. Doyle, D. A. Allen, and J. Elias. Ground-based near-infrared imaging observations of Venus during the Galileo encounter. *Science,* 2.53:1538-1541, 1991.

Crisp, D., V. S. Meadows, D. A. Allen, B. Bézard, C. de Bergh, J.-P. Maillard, Near-infrared oxygen airglow from the Venus nightside. The *International Colloquium on Venus, Pasadena, CA 10-12 August 1992, 23-24, 1992.*

Dickinson, R. E., and E. C. Ridley. A numerical model for the dynamics and composition fo the Venusian thermosphere. *J. Atmos. Sci.*, 32:1219-1231, 1975.

Dickinson, R. P., and E. C. Ridley. Venus mesosphere and thermosphere temperature structure, II, day-night variations. *Icarus,* 30:163, *1977.*

Drossart, P., B. Bézard, Th. Encrenaz, E. Lellouch, M. Roos, F. W. Taylor, A. D. Collard, S. B. Calcutt, J. B. Pollack, D. H. Grinspoon, R. W. Carlson, K. H. Baines, and L. W. Kamp. Search for spatial variations of the H_20 abundance in the lower atmosphere of Venus from NIMS-Galileo. *Planet. Space Sci., 41* (7):495-*504,* 1993.

Fox, J. L. and S. W. Bougher. Structure, luminosity, and dynamics of the Venus thermosphere. *Space* Sci. Rev., 55:357-489, 1991.

Gillingham, P. R., and A. Lankshear. *Proc. SPIE*, 1235:9, 1991.

Goldstein, J. J., M. J. Mumma, T. Kostiuk, D. Deming, F. Espenak, and D. Zipoy. Absolute wind velocities in the lower thermosphere of Venus using infrared heterodyne spectroscopy. *Icarus,* 94:45-63, 1991.

Greene, T. P., A. T. Tokunaga, D. W. Toomey, and J. S. Carr. CSHELL: A high spectral resolution 1-5 micron cryogenic echelle spectrograph for the IRTF. *Infrared Detectors and Instrumentation, A. M. Fowler editor, Proc. SPIE*, 1946:313-324, 1993.

Huestis, D. L. and T. G. Slanger. New perspectives on the Venus nightglow. *J. Geophys.*

Res., 98(E6):10839- 10847, 1993.

Krasnopol'sky, V. A. Venus spectroscopy in the 3000-8000 angstrom region by Veneras 9 and 10. In D. M. Hunten, L. Colin, T. M. Donahue, and V. 1. Moroz, editors, *Venus*, pages 459-483, 1983.

Lellouch, E., J. J. Goldstein, J. Rosenquist, S. W. Bougher, and G. Paubert. Global circulation, thermal structure, ant] carbon-monoxide distribution in the Venus mesosphere in 1991. *Icarus*, 110:315-339, 1994.

Leu, M. T., and Y. L. Yung. Determination of' $O_2(a^1\delta_g)$ and $O_2(b^1\sigma_g^+)$ yields in the reaction O + C]() $\rightarrow$ Cl + O_2 : implications for photochemistry in the atmosphere of Venus. *Geophys. Res. Lett.*, 14:949-952, 1987.

Lieu, K. N. *An Introduction to Atmospheric Radiation.* Academic Press, Inc, 1980.

Maillard, J.-1'., B. Bezard, L. Domisse, D. Crisp, and D. Simons. Spectro-imaging of the dark side of Venus in the 1.27pm 0_2 emission with an imaging 1"'1'S. Bull. *Am. Astron. Sot.*, 25:1095, 1993.

Maillard, J. P. and D. Simons. First results of an imaging FTS with a NICMOS camera.]n *Proceedings of an ESA Workshop on Solar Physics and Astrophysics at Interferometric Resolution*, pages 205-210, 1992.

Meadows, V. S. PhD thesis, University of Sydney, 1994.

Meadows, V. S., and D. Crisp. Ground-based near-infrared observations of the Venus nightside: 'The thermal structure and water abundance near the surface. *J. Geophys. Res.*, *1995.* this issue.

Na, C. Y., L. W. Esposito, and T. E. Skinner. International Ultraviolet Explorer observation of Venus $S0_2$ and S(). *J. Geophys. Res.*, 95(D6):7485–7491, 1990.

Na, C. Y., L. W. Esposito, W. E. McClintock, and C. A. Barth. Sulfur-dioxide in the atmosphere of Venus 2. Modeling results. *Icarus*, 112:389 395, 1994.

Noxon, J. F., W. A. Traub, N. P. Carleton, and P. Connes. Detection of O_2 dayglow emission from Mars and the Martian ozone abundance. *Ap. J.*, 207:1025-1035, 1976.

Parisot, J. P., and G. Moreels. Oxygen 1.27-μm emission from the atmosphere of Venus. *Icarus*, 42:46 53, 1980.

Rothman, L. S. Magnetic dipole infrared atmospheric oxygen bands. *Appl. Optics*, 21 (13):2428-2431, 1982.

Seiff, A., D. B. Kirk, R. E. Young, R. C. Blanchard, J. 'T. Findlay, G. M. Kelly, and S. C. Sommer. Measurements of thermal structure and thermal contrasts in the atmosphere of Venus and related dynamical observations: Results from the four 1 'ioneer Venus probes. *J. Geophys. Res.*, 85(AI 3) :7903-7333, 1980.

Shah, K. 1'., 1). O. Muhleman, and G. L. Berg-c. Measurement of winds in Venus' upper mesosphere based on Doppler shifts of the 2.&ml n ^{12}CO line. Icarus, 93:96-121, 1991.

Stamnes, K., S. C. Tsay, W. Wiscombe, and K. Jayaweera. Numerically stable algorithm for discrclm-ordinat,c-method radiative transfer in multiple scattering and emitting layered media. *Appl. Optics*, 27(12):2502–2509, 1988.

Stewart, A. I. F., J. C. Gérard, D. W. Rusch, and S. W. Bougher. Morphology of the Venus ultraviolet night airglow. *J. Geophys. Res.*, 85(AI 3) :7861-7870, 1980.

Taylor, F. W., R. Beer, M. T. Chahine, I). J. Diner, L. S. Elson, R. D. Haskins, D. J.

McCleese, J. V. Martonchik, P. E. Reichley, S. P. Bradley, J. Delderfield, J. T. Schofield, C. B. Farmer, L. Froidevaux, J. Leung, M. T. Coffey, and J. C. Gille. Structure and meteorology of the middle atmosphere of Venus: Infrared remote sensing from the Pioneer Orbiter. *J. Geophys. Res.*, 85(A13):7963 8006, 1980.

Trauger, J. T. and J. I. Lunine. Spectroscopy of molecular oxygen in the atmospheres of Venus and Mars. *Icarus*, 55:272-281, 1983.

Yung, Y. L. and W. B. DeMore. Photochemistry of the stratosphere of Venus: Implications for atmospheric evolution. *Icarus*, 51:199 247, 1982.